

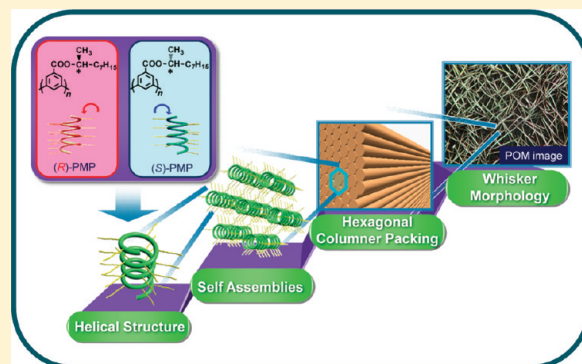
Self-Assembled Helical Conjugated Poly(*m*-phenylene) Derivatives That Afford Whiskers with Hexagonal Columnar Packed Structure

Kiyoshi Suda and Kazuo Akagi*

Department of Polymer Chemistry, Kyoto University, Katsura, Kyoto 615-8510 (Japan)

Supporting Information

ABSTRACT: We have synthesized a series of π -conjugated polymers, poly(*m*-phenylene) [PMP] derivatives with chiral or racemic alkyl groups in side chains. Peculiar liquid crystalline phases or crystalline structures based on helical conjugated polymer main chains are elucidated. The PMPs synthesized by polymerizations of chiral and racemic monomers are found to self-assemble to form whiskers, so far as the polymers bear secondary alkyl groups with appropriate lengths in side chains. The whiskers have a hexagonal columnar packed structure, and the columns are uniaxially aligned parallel to the long axis of the whisker. The measurements of circular dichroism spectra and X-ray diffractions indicate that the polymers have a one-handed helical structure consisting of helicene-type conjugated main chains. The chiral PMPs show not only linearly polarized fluorescence after the macroscopic alignment but also circularly polarized fluorescence owing to the helical conjugated main chain.



1. INTRODUCTION

The whisker of the polymer is a spontaneously formed assembly with a higher-order structure and could be used as a single fiber serving for amplified intrinsic properties of the polymer. The whiskers of aromatic polyesters such as poly(*p*-oxybenzoyl) and poly(2-oxo-6-naphthoyl) have been intensively investigated,¹ while there have been few reports on the whiskers of conjugated polymers except poly(3-alkylthiophene).² The whisker of poly(3-alkylthiophene) is composed of self-assembled planar conjugated chains stacked along the long axis of the polymer, yielding laminated layers separated by alkyl side chains. However, no whisker consisting of self-assembled helicene-like helical conjugated chains has been put forward until now. When the helical conjugated polymer giving the whisker structure is designed, the intrachain and interchain interactions must be balanced by precisely controlling van der Waals, π -overlap, and electrostatic interactions.

The helical conjugated polymers have been attracting much interest because they could provide us with not only unique optical functions such as circularly polarized luminescence³ and nonlinear second harmonic generation,⁴ but also unprecedented physicochemical properties such as an induced solenoidal magnetism.⁵ Various kinds of helical conjugated polymers represented by helical polyacetylenes,⁶ amino acid-containing substituted polyacetylene derivatives,⁷ poly(phenylacetylene) derivatives,⁸ and polythiophene derivatives⁹ have been reported. These helical conjugated polymers are constructed with intrachain-spiral, intrachain-twisted ribbon, or interchain-helicity π -stacked structures.¹⁰ However, there are a few reports of the conjugated polymers having a helicene-like helical structure,^{11–14} which is favorable for maintaining

π -conjugation on the main chain despite of the intrachain helical structure. The *m*-phenylene fragment is likely a building block suitable for construction of helicene-like helical structure because of its ability to form a *cis* linkage between the 1 and 5 positions of the phenylene ring. This hypothesis is supported by previous studies showing that *m*-phenylethyne oligomers spontaneously form helical structures depending on solvent and temperature,¹² and that the *m*-deciphenyl compound¹³ and poly(*m*-phenylene)¹⁴ have helical structures where each turn of the helix has five aromatic rings.

In this study, we designed and synthesized a series of novel poly(*m*-phenylene) [PMP] derivatives with chiral or racemic groups in the side chains. The PMPs have helicene-like helical structures through intrachain π -electron overlaps. The PMPs self-assemble to form whiskers when slowly cooled from the isotropic phase irrespective of presence of chirality in the side chains. X-ray diffraction (XRD) analyses indicate that the whisker is composed of a hexagonal columnar packing of the helical main chains. The formation of the whisker is the first example among the helical π -conjugated polymers reported so far.

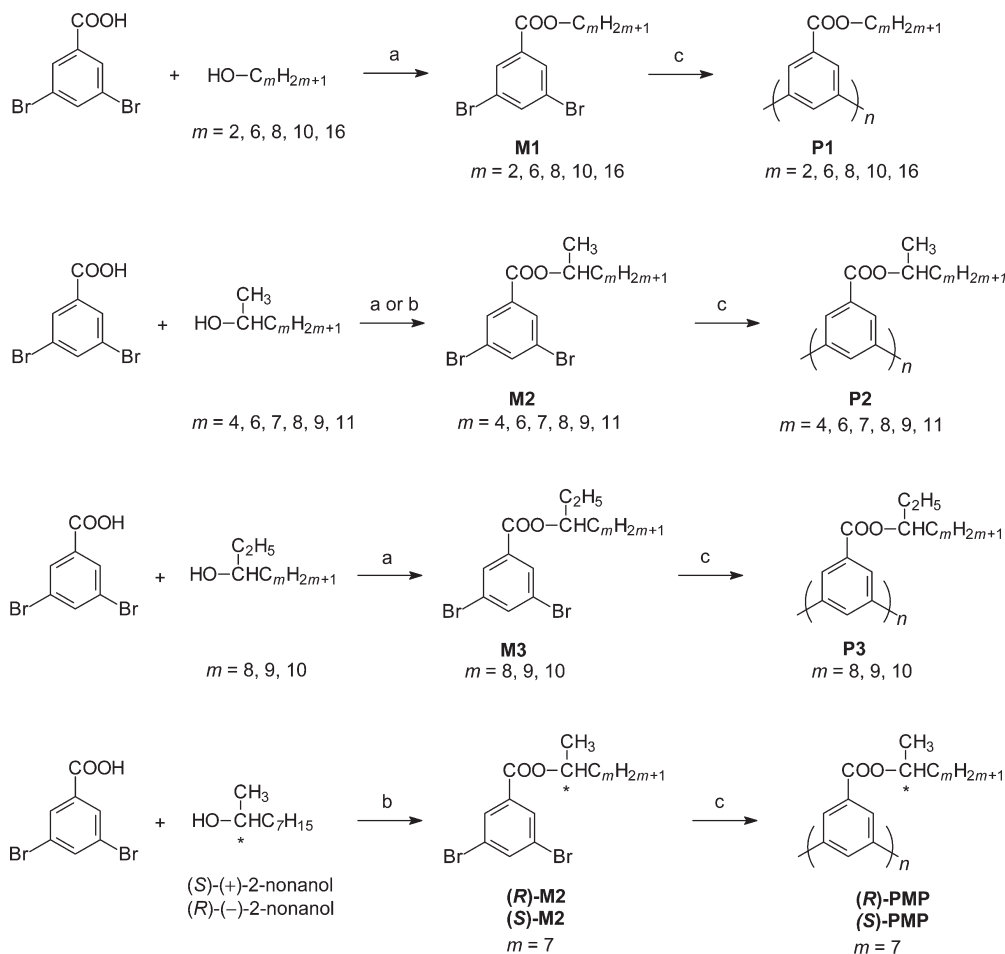
2. SYNTHESSES

2.1. Materials. All the reagents were commercially available and used without further purification. 3,5-Dibromobenzoic acid, 2,2'-bipyridine, (\pm)-2-nonanol, diethyl azodicarboxylate (DEAD)

Received: August 12, 2011

Revised: November 1, 2011

Published: November 21, 2011

Scheme 1. Synthetic Routes of Monomers and Polymers^a

^aKey: (a) DCC, DMAP, CH₂Cl₂. (b) DEAD, TPP, THF. (c) Ni(cod)₂, bpy, DMF. DCC: *N,N'*-dicyclohexylcarbodiimide. DMAP: *N,N*-dimethylaminopyridine. DEAD: diethylazodicarboxylate. TPP: triphenylphosphine. Ni(cod)₂: bis(1,5-cyclooctadiene)nickel(0). bpy: 2,2'-bipyridyl.

(40 wt % solution in toluene), 1-hexanol, 1-octanol, 1-decanol, 1-hexadecanol, 2-hexanol, 2-octanol, 2-nonanol, 2-decanol, 2-undecanol, 2-tridecanol, 3-nonanol, 3-decanol and 3-undecanol were purchased from Tokyo Kasei Co. Ltd. (S)-(+)-2-Nonanol, (R)-(-)-2-nonanol, and triphenylphosphine (TPP) were purchased from Wako Co. Ltd. Nickel acetylacetonate was purchased from Kanto Chemical Co. Ltd. Bis(1,5-cyclooctadiene)-nickel(0) [Ni(COD)₂] was prepared by the literature procedure.¹⁵ THF and DMF were dried over sodium and potassium hydroxide, respectively, and distilled prior to use. All experiments were performed under an argon atmosphere.

2.2. Syntheses of polymers. Poly(*m*-phenylene) derivatives, whose side chains are composed of various lengths of primary and secondary racemic alkyl groups, and chiral (R)-(-)- or (S)-(+)-1-methyloctyl group, were synthesized by following steps (Scheme 1).

Esterification of 3,5-dibromobenzoic acid was carried out in ethanol in the presence of small amount of sulfuric acid to give a dibrominated precursor, ethyl 3,5-dibromobenzoate (**M1**, *m* = 2). Polymerizations of **M1** (*m* = 2) was carried out in DMF by dehalogenation polycondensations, where Nickel chloride was reduced to give nickel(0) complex in the presence of zinc powder and 2,2'-bipyridyl.

Other esterifications of 3,5-dibromobenzoic acid with long primary and secondary alcohols or chiral (R)-(-)- and (S)-(+)-2-nonanol

were carried out using dicyclohexylcarbodiimide (DCC) and *N,N*-dimethylaminopyridine (DMAP), or diethyl azodicarboxylate (DEAD) and triphenylphosphine (TPP), to give corresponding dibrominated precursors, **M1** (*m* = 6, 8, 10 and 16), **M2** (*m* = 4, 6, 7, 8, 9 and 11), **M3** (*m* = 8, 9 and 10), and (R)-**M2** (*m* = 7) and (S)-**M2** (*m* = 7), as yellow to colorless oil in good yields.¹⁶ The stereochemistry of the chiral alcohol of the resulting precursor changes into the opposite configuration through a Walden's inversion in an S_N2 reaction. Polymerizations of the precursors were carried out at 100 °C in *N,N*-dimethylformamide using Ni(COD)₂ to give the corresponding poly(*m*-phenylene) derivatives [**P1**, **P2**, **P3**, (R)-**PMP** and (S)-**PMP**] with good yields (89–99%).¹⁷ Here it should be noted that strictly speaking, (R)- and (S)-**PMP** have homochiral side chains and **P2** and **P3** have stereochemically random side chains with no optical activity. For the sake of simplicity, however, (R)- and (S)-**PMP** are represented as the polymers having chiral side chains throughout the manuscript.

3. RESULTS AND DISCUSSION

3.1. Molecular Weights and Thermal Properties. All the polymers were soluble in common organic solvents such as THF, CHCl₃ and *n*-hexane, while they were fusible, except for **P1**

Table 1. Molecular Weights, Dispersion Ratio, and Degrees of Polymerization Calibrated with Polystyrene Standard Using THF as an Eluent^a

| polymer | <i>m</i> | <i>M_n</i> | <i>M_w</i> | <i>M_w/M_n</i> | D.P. * |
|------------------|----------|----------------------|----------------------|------------------------------------|--------|
| P1 | 2 | 2100 | 2900 | 1.3 | 14 |
| | 6 | 2300 | 3000 | 1.3 | 11 |
| | 8 | 2300 | 6200 | 2.6 | 10 |
| | 10 | 2800 | 3700 | 1.3 | 11 |
| | 16 | 3700 | 5400 | 1.5 | 11 |
| P2 | 4 | 2100 | 3200 | 1.5 | 10 |
| | 6 | 3000 | 11 100 | 3.7 | 13 |
| | 7 | 3500 | 6200 | 1.7 | 14 |
| | 8 | 3100 | 4400 | 1.4 | 12 |
| | 9 | 3000 | 12 400 | 4.1 | 11 |
| P3 | 11 | 3600 | 6700 | 1.9 | 12 |
| | 8 | 2800 | 4000 | 1.4 | 11 |
| | 9 | 2000 | 4000 | 2.0 | 8 |
| | 10 | 2100 | 3700 | 1.8 | 8 |
| (<i>R</i>)-PMP | 7 | 3500 | 6200 | 1.7 | 14 |
| (<i>S</i>)-PMP | 7 | 3700 | 6600 | 1.8 | 15 |

^a *M_n*: number-average molecular weight. *M_w*: weight-average molecular weight. *M_w/M_n*: degree of dispersion. DP: degree of polymerization.

(*m* = 2). The molecular weights of the polymers were evaluated with gel permeation chromatography (GPC) calibrated with polystyrene standard. As summarized in Table 1, number-average molecular weights of the polymers were 2000–3700 and the degrees of polymerizations (DPs) were 8–15. The DP in each type of the polymer (P1–P3) tends to gradually decrease with increasing the alkyl length (*m*) of side chain. It is probably due to the steric hindrance of the polymer side chains between neighbor units. All the polymers allowed us to prepare cast films by casting the polymer solution onto substrates.

Introduction of a longer aliphatic chain into the side chains leads to decreases in both melting and clearing points of the polymers, as already confirmed in several cases of calamitic (rod-shaped liquid crystalline) compounds.¹⁸ Upon slowly cooling the polymers from the isotropic phases, they showed peculiar optical textures, as depicted in Figure 1. The thermal behaviors of the polymers were evaluated by DSC analyses and POM observations. The phase transition temperatures of the polymers are summarized in Table 2.

The polymers with primary alkyl side chains, P1 (*m* = 6–16), exhibited mosaic textures characteristic to discotic columnar phases.¹⁹ The domain seems rounded in cases of P1 (*m* = 6–10), but squared in a case of P1 (*m* = 16). It should be noted that only P1 (*m* = 16) showed intense DSC peaks at 32 and 29 °C in the heating and cooling process, respectively, indicating an occurrence of the second phase transition. The phase transition temperatures were lowered with an increase of the chain lengths. This may be due to the fact that the self-assembled polymers in the meso phase are more flexible and fusible when the alkyl chains are incorporated to the side chains.²⁰

The phase transition temperatures of P2 with the secondary alkyl side chains are slightly lower than those of P1 with the primary alkyl side chains, probably due to smaller interactions between the branched side chains. The polymers with methyl branched longer alkyl groups, P2 (*m* = 6–8), showed whisker morphologies when slowly cooled from the isotropic phases.^{21,22}

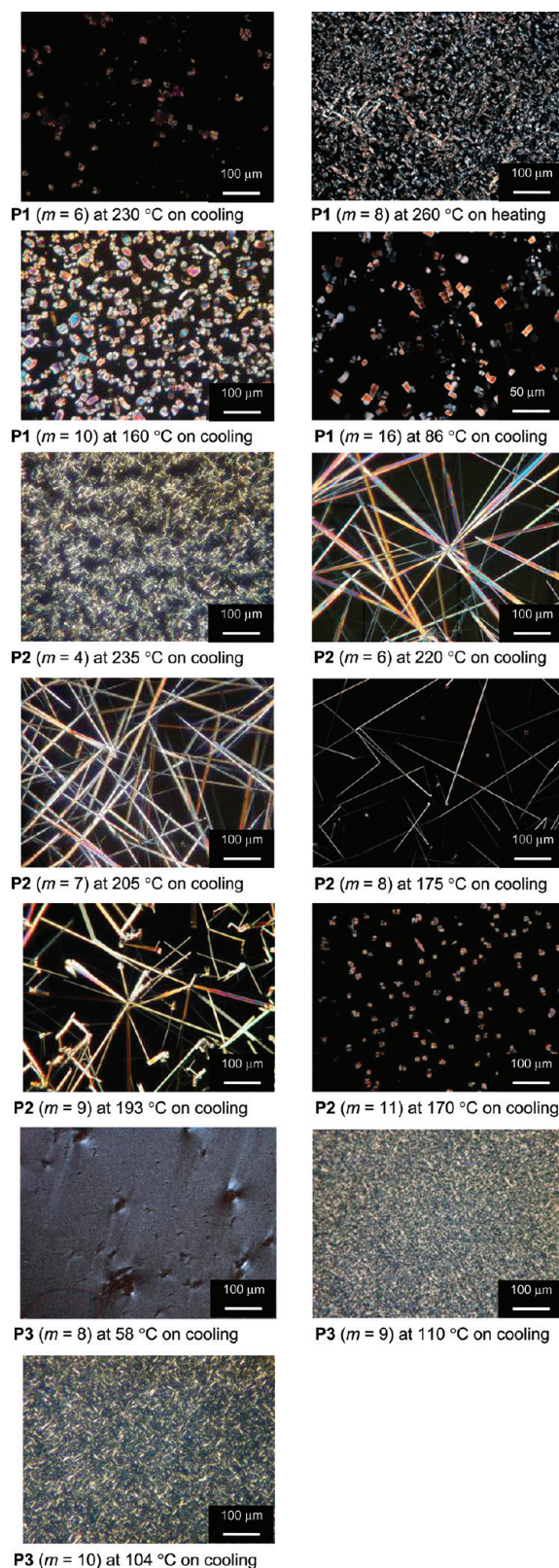


Figure 1. Polarized optical micrographs of the poly-*m*-phenylene (PMP) polymers.

It seems necessary to have both methyl branched structure and an appropriate carbon chain length from 7 to 9 for the formation of the whisker morphology. Actually, P2 (*m* = 9) showed a bent

Table 2. Phase Transition Temperatures and Characterizations of the PMP Polymers^a

| polymer | <i>m</i> | heating (°C)/cooling (°C) | | |
|---------|----------|------------------------------------------------------------------------------------------------|----------------------------------------------------------------|--------------------------------------------------------------|
| P1 | 2 | <i>b</i> | | |
| | 6 | S 158 Col _h 250< I S 130 Col _h 250< I | | |
| | 8 | S 152 Col _h 250< I S 126 Col _h 250< I | | |
| | 10 | S 131 Col _h 209 I S 106 Col _h 182 I | | |
| | 16 | S 26 D _L 32 Col _h 115 I S 20 D _L 29 Col _h 110 I | | |
| | P2 | 4 | S 126 Col _h 250< I S 120 Col _h 250< I | |
| | | 6 | S 158 Col _h 231 I S 110 Col _h 208 I | |
| 7 | | S 126 Col _h 210 I S 117 Col _h 205 I | | |
| 8 | | S 127 Col _h 197 I S 114 Col _h 170 I | | |
| 9 | | S 126 Col _h 206 I S 112 Col _h 193 I | | |
| 11 | | S 118 Col _h 191 I S 110 Col _h 164 I | | |
| P3 | | 8 | S 37 Col _h 66 I S 33 Col _h 58 I | |
| | | 9 | S 99 Col _h 145 I S 95 Col _h 127 I | |
| | | 10 | S 91 Sm 131 I S 86 Sm 114 I | |
| | | (R)-PMP | 7 | S 126 Col _h 210 I S 117 Col _h 205 I |
| | | | (S)-PMP | 7 |

^a S: solid state. Col_h: hexagonal columnar structure. D_L: discotic lamellar structure. Sm: smectic liquid crystalline phase. I: isotropic phase.

^b Infusible.

whisker, whereas P2 (*m* = 11) gave no whisker but a fan shaped texture.

The polymer with ethyl branched octyl group in side chain, P3 (*m* = 8), showed a homogeneously bright texture at 58 °C on cooling from the isotropic phase. The polymers with ethyl branched longer alkyl (nonyl and octyl) groups, P3 (*m* = 9, 10), showed batonnet textures that resemble to the textures of smectic liquid crystalline polymers. As seen in Table 3, P3 (*m* = 8) has relatively lower phase transition temperatures. This may be due to a larger steric repulsion between the side chains, which decreases a thermal stability of the polymers with self-assembled hexagonal columnar (Col_h) structure. Thus, the morphologies of the PMP derivatives crucially depend on the bulkiness and lengths of the side chains.

The PMPs with chiral alkyl groups in the side chains [(R)-PMP and (S)-PMP] were subsequently synthesized. The average molecular weights (*M_n*) of (R)-PMP and (S)-PMP were 3500 and 3700, respectively, and the degrees of polymerizations (DPs) were 14 and 15, respectively. It is found that these racemic polymers also form whiskers when slowly cooled from the isotropic

phase, as depicted in Figure 2. The whiskers observed for the present PMPs have 5–7 μm in diameter and about 100–200 μm in length. The size of the whisker depends on not only the polymer structure including side chains but also the cooling rate from the isotropic phase. Large area of the POM micrograph is dark, but the circularly polarized micrograph indicates that the dark area even contains many whiskers (Figure 2b).

It is useful to remark here that P2 (*m* = 7) is analogous to the (R)-PMP and (S)-PMP and that it also forms whiskers whose morphology is very similar to those of (R)-PMP and (S)-PMP (see Figure 1 and Figure 2). P2 (*m* = 7) is synthesized by the polymerization of racemic monomer, M2 (*m* = 7), and it can be regarded as a polymer bearing a stereochemically random side chains with no optical activity but not as a racemic PMP. This is because P2 (*m* = 7) should include (R)-PMP and (S)-PMP and even the diastereomers having segments mixed with (R) and (S)-*m*-phenylene units. Thus, it is worthwhile to note that the whiskers of PMP might be formed through not only the self-assembly of the chiral PMPs but also that of the diastereomers of PMP.

3.2. X-ray Diffraction Analysis. The structures of the polymers in crystalline phases were investigated by X-ray diffraction (XRD) measurements. The XRD results and the assignments of the structures are summarized in Table 3. Schematic representation of stacking structures for PMP derivatives is shown in Figure 3.

P1 (*m* = 2) showed an intense peak corresponding to the distance of 17.1 Å and weak peaks of 9.5, 8.3, 6.2, and 5.4 Å having the reciprocal Bragg spacing in ratios of 1:√3:2:√7:3:√13:4. These peaks are respectively assigned to Miller indices of (100), (110), (200), (210), and (300) reflections of hexagonal arrangement with a lattice constant of *a* = 19.7 Å.^{23–26} The result suggests that P1 (*m* = 2) is a hexagonal columnar (Col_h) crystal structure consisting of helical main chains with *cisoid* linkages. In addition, the peak of 3.6 Å, that is coincident with the typical distance for π–π stacking between aromatic rings of the helical pitches, was also observed in the wide angle region (Figure S2, in Supporting Information).^{21,25,27} This means that the lamination of the aromatic units is ordered along the columnar axis, as reported for the crystalline phase of triphenylene derivatives.²⁸ Similarly, P1 (*m* = 6–10) showed intense peaks around 21–25 Å and some diffraction peaks based on the Col_h structure. The lattice parameters corresponding to the distances between the columns increase with increasing the alkyl lengths of the side chains. The broad halos around 4.1–4.6 Å are related to disordered alkyl chains.²⁶ Since P1 (*m* = 16) has two phases in the crystal state, the temperature dependence of XRD profile of the polymer was examined. At higher temperature, the polymer showed diffractions of 30.3, 17.7, 15.3, 11.2, 10.3, 8.4, 8.2, and 7.9 Å, that correspond to the reciprocal Bragg spacings in ratios of 1:√3:2:√7:3:2√3:√13:4 of Col_h phase with a lattice constant of 35.0 Å; At the lower temperature (below 29 °C), the polymer showed diffraction peaks of 33.5, 16.8, 11.3, and 8.3 Å, that are proportional to the reciprocal ratios of 1:2:3:4. These peaks are assigned to (001), (002), (003), and (004) of a discotic lamellar (D_L) phase with a lattice parameter of 33.6 Å.²⁹ On the other hand, the intense peak of 4.2 Å is assigned to a lamellar structure of the alkyl group. It is understood that the introduction of the long alkyl groups in the side of PMP leads to a drastic change from the Col_h to the D_L structure.

P2 (*m* = 4) showed diffraction peaks of 19.8, 11.3, 9.7, 6.4, and 5.3 Å, that are respectively assigned to Miller indices of (100),

Table 3. Crystal Structures and Lattice Parameters of PMP Polymers^a

| polymer | <i>m</i> | lattice parameter/Å | diffraction distance/Å (Miller indices) | phase |
|---------|-----------------|---------------------|------------------------------------------------------------------------------------------|------------------|
| P1 | 2 ^b | 19.7 | 17.1 (100), 9.5 (110), 8.3 (200), 6.2 (210), 5.4 (300), 3.6 | Col _h |
| | 6 | 24.3 | 21.4 (100), 12.1 (110), 10.4 (200), 8.0 (210), 7.0 (300), 4.1, 3.7 | Col _h |
| | 8 | 26.4 | 23.5 (100), 13.2 (110), 11.5 (200), 8.6 (210), 7.6 (300), 4.6, 3.7 | Col _h |
| | 10 | 28.3 | 25.0 (100), 14.3 (110), 12.0 (200), 9.2 (210), 8.1 (300), 4.5, 3.7 | Col _h |
| | 16 ^c | 35.0 | 30.3 (100), 17.7 (110), 15.3 (200), 11.2 (210), 10.3 (300), 4.3 | Col _h |
| | | 33.6 | 33.5 (100), 16.8 (200), 11.3 (300), 8.3 (400), 4.2, 3.7 | D _L |
| P2 | 4 | 22.5 | 19.8 (100), 11.3 (110), 9.7 (200), 6.4 (300), 5.3 (310), 4.1, 3.7 | Col _h |
| | 6 | 26.4 | 23.5 (100), 13.3 (110), 11.3 (200), 8.6 (210), 6.5 (220), 4.1, 3.7 | Col _h |
| | 7 | 27.1 | 23.8 (100), 11.9 (200), 8.7 (210), 7.8 (300), 6.5 (310), 4.1, 3.7 | Col _h |
| | 8 | 27.2 | 24.4 (100), 12.2 (200), 9.1 (210), 8.1 (300), 6.7 (310), 4.1, 3.7 | Col _h |
| | 9 | 28.7 | 24.9 (100), 12.4 (200), 9.3 (210), 8.3 (300), 6.9 (220), 4.1, 3.7 | Col _h |
| | 11 | 28.9 | 25.0 (100), 12.0 (200), 9.0 (210), 7.9 (300), 4.1, 3.7 | Col _h |
| P3 | 8 | 26.8 | 23.2 (100), 13.8 (110), 11.6 (200), 9.4 (210), 7.7 (300), 4.4, 3.7 | Col _h |
| | 9 | 28.7 | 24.1 (100), 18.4 (110), 12.0 (200), 8.8 (210), 7.9 (300), 4.4, 3.7 | Col _h |
| | 10 | 24.4 | 24.4 (100), 12.2 (200), 8.2 (300), 6.1 (400), 4.5, 3.7 | Sm |
| (R)-PMP | 7 | 27.5 | 23.5 (100), 13.6 (110), 11.8 (200), 8.8 (210), 7.8 (300), 6.7 (310), 5.8 (400), 4.4, 3.7 | Col _h |
| (S)-PMP | 7 | 27.5 | 23.5 (100), 13.8 (110), 11.8 (200), 8.8 (210), 7.7 (300), 6.5 (310), 5.8 (400), 4.4, 3.7 | Col _h |

^a Col_h: hexagonal columnar structure. D_L: discotic lamellar structure. Sm: smectic liquid crystalline phase. ^b Infusible. ^c P1 (*m* = 16) shows Col_h and D_L phases at higher and lower temperatures, respectively, between isotropic and solid states.

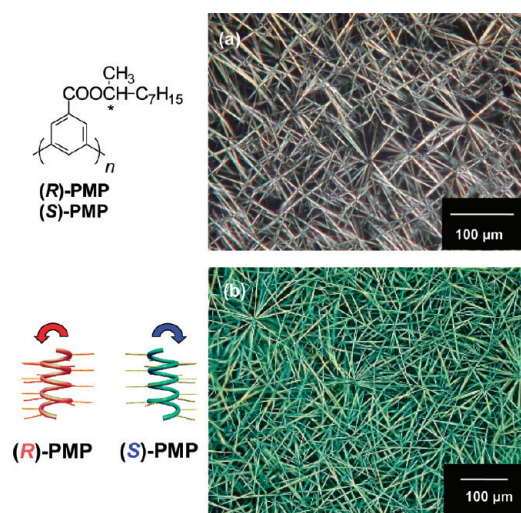


Figure 2. (a) Polarized optical micrograph and (b) circularly polarized optical micrograph of (R)-PMP in the solid state.

(110), (200), (300), and (310) of Col_h with a lattice constant of $a = 22.5$ Å. Besides, the peak of 4.1 Å, assigned to the distance between π - π stacking corresponding to the helical pitch, was observed in the wide angle region. Similar diffraction patterns were also observed in other P2 (*m* = 6–11) polymers having the whisker textures.

P3 (*m* = 8 and 9) showed the diffraction patterns of Col_h phase with lattice constants of 26.8 and 28.7 Å, respectively. The diffractions with the index of (100) became narrowed with lengthening of the side chain. The result suggests that the hexagonal packing is strengthened by the introduction of the bulky side chains, leading to an enhancement in ordering of the stacking along the columnar axis. Furthermore, P3 (*m* = 10) with the longer side chain showed diffractions of 24.4, 12.2, 8.2, and 6.1 Å in the short angle region where the reciprocal Bragg

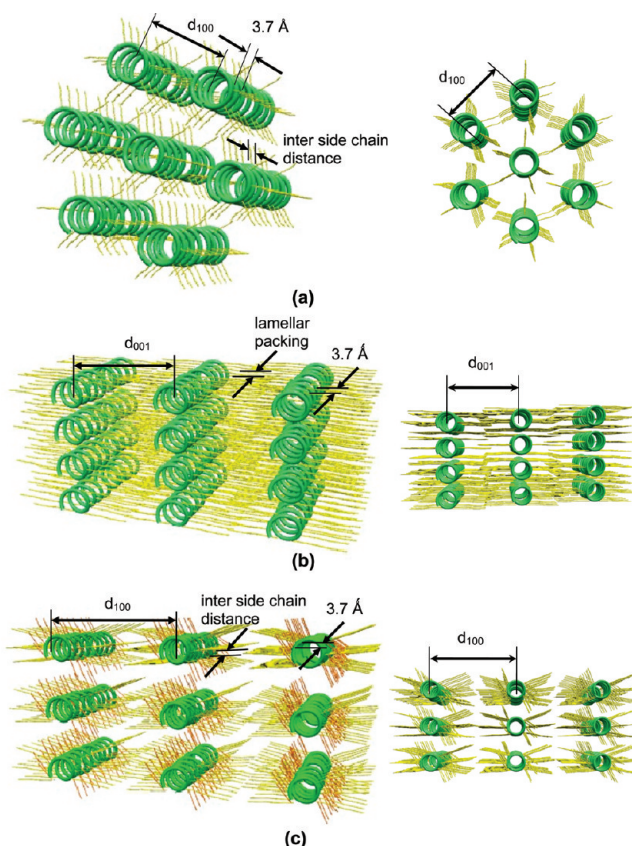


Figure 3. Schematic representation of stacking structures of PMP polymers: (a) hexagonal columnar (Col_h), (b) discotic lamellar (D_L), and (c) smectic (Sm) liquid crystalline structures.

spacings are in ratios of 1:2:3:4. Such an integral diffraction pattern seemingly looks like that of the D_L phase. However, only a broad halo at 4.5 Å and a shoulder peaks at 3.7 Å were

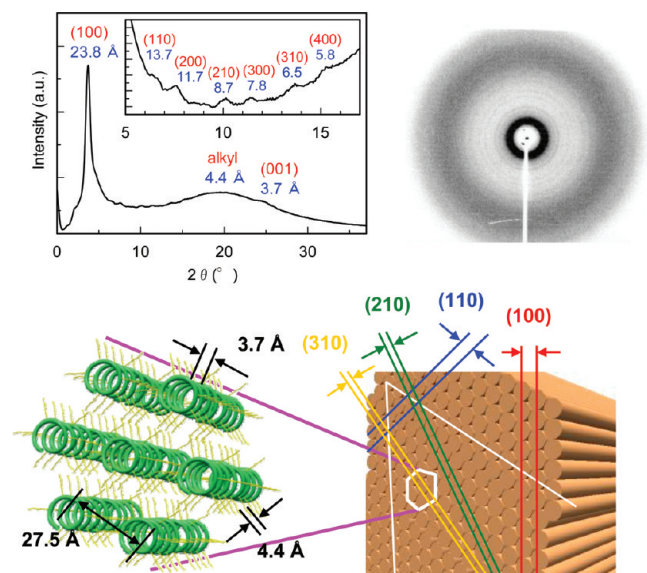


Figure 4. X-ray diffraction profile and pattern of (*R*)-PMP at the solid state. Inset shows the expanded XRD profiles in the region of $5\text{--}17^\circ$ in 2θ . The assignments for hexagonal columnar (Col_h) crystal are given in the schematic figure of self-assembled polymers.

observed in the wide angle region, indicating an absence of the lamellar structure. Hence, this diffraction pattern could be assigned to a smectic phase (Sm) with a layer distance of 24.4 \AA .³⁰ Note that the side chains of the polymers in the D_L phase are slightly interdigitated, whereas those in the Sm phase are not interdigitated but separated to each other, as shown in Figure 3.

It is of interest that the polymers with chiral side chains have XRD results similar to those of the polymers with stereochemically random side chains. Figure 4 shows the XRD profile and pattern of (*R*)-PMP at the solid state. (*R*)-PMP shows an intense peak at 23.8 \AA and six weak peaks at 13.7 , 11.7 , 8.7 , 7.8 , 6.5 , and 5.8 \AA in the small angle region. A diffuse halo is present at 4.4 \AA , and a sharp but small halo is present at 3.7 \AA in the wide angle region. The peaks that represent the reciprocal Bragg spacings with ratios of $1:\sqrt{3}:2:\sqrt{7}:3:\sqrt{13}:4$ were assigned to Miller indices of (100), (110), (200), (210), (300), (310), and (400), respectively. The reflections have a hexagonal arrangement with a lattice constant of $a = 27.5 \text{ \AA}$.^{27,31} The diffuse peak in the wide angle region (4.4 \AA) corresponds to the distance of the side chains.²⁵ The periodicity of 3.7 \AA corresponds to the distance between the π -stacks of the phenylene cores.^{21,25,27} These results show that the polymer has a helicene-like helical structure with a helical pith of 3.7 \AA .^{21,23,24}

The XRD profile of (*R*)-PMP is similar to those of columnar discotic liquid crystals^{21,23,24} and helicenes.^{25,26} In fact, the molecular mechanics (MM) calculations indicate that the helix is composed of six repeating units, and the diameter is estimated to be 25 \AA . This estimate is in agreement with the experimental results (27.5 \AA) obtained from the XRD measurements.³² The aromatic cores are not tilted with respect to the columnar axis. The order of the whisker remains unchanged even in the solid state.²⁸ Similar XRD results were obtained for (*S*)-PMP. Hence, the whisker has a hexagonal columnar (Col_h) structure consisting of discotically packed helical conjugated polymers, as also illustrated in Figure 4.

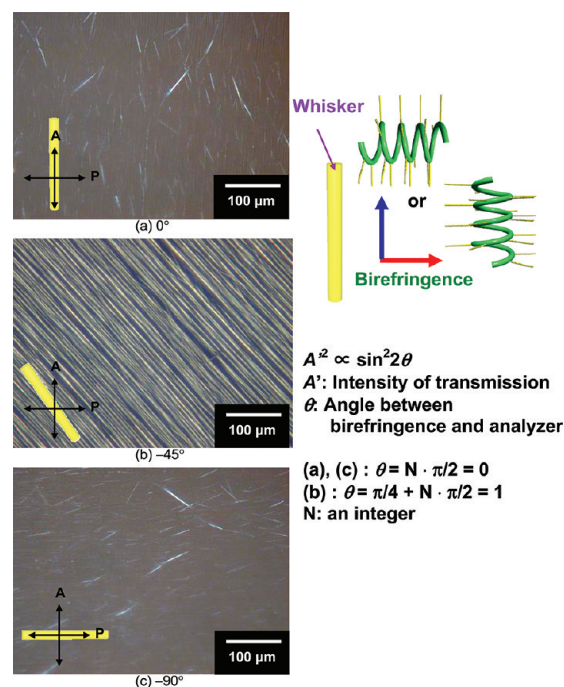


Figure 5. POM photographs of (*R*)-PMP: (a) solid state of the polymer on an orientated substrate (orientated direction is vertical one); (b) the sample is rotated by -45° from the position in part a; (c) the sample is rotated by -90° from the position in part a.

3.3. Polarizing Optical Micrographs (POMs). To examine how the columns of the PMP helices are organized to form a whisker with hexagonal structure, the direction of birefringence and the refractive index were investigated through POM measurements (Figures 5 and 6). The whiskers were aligned by slowly cooling the polymer on an oriented substrate from an isotropic to a solid state, so that the axes of the whiskers were aligned parallel to the orientation direction of the substrate. The optical texture of the polymer was well preserved even in the solid state.

When the long axis of the whisker is placed parallel or perpendicular to the direction of the analyzer, the anisotropic region darkens because the optical axis of the whisker coincides with the plane of polarization (Figure 5a). After the sample was rotated -45° from the dark position, a bright area representing a diagonal position was observed (Figure 5b). Further rotation of the sample by -45° from the bright area produced a dark image (Figure 5c). The result indicates that the columns of the helices for the PMPs are uniaxially aligned parallel to the long axes of the whiskers.²⁴

The refractive indexes of the whisker were next investigated by examining changes in the interference colors. The changes in the interference colors were observed with a retardation plate ($\lambda = 530 \text{ nm}$). The aligned sample (the whisker) and the retardation plate ($\lambda = 530 \text{ nm}$) were set between the polarizer and analyzer. The interference color was evaluated by changing the relative angle between the retardation plate and the sample, as shown in Figure 6. The interference color depends on the retardation (R) of the light, where the retardation is the product of the thickness (d) and the difference (Δn) of refractive index of the sample; $R = d\Delta n$, where $\Delta n = n_{\parallel} - n_{\perp}$. The retardation plate is arranged parallel to the sample (see Figure S6 in Supporting Information). In this case, when the interference color is blue, the Δn is negative. This indicates that the refractive index (n_{\parallel})

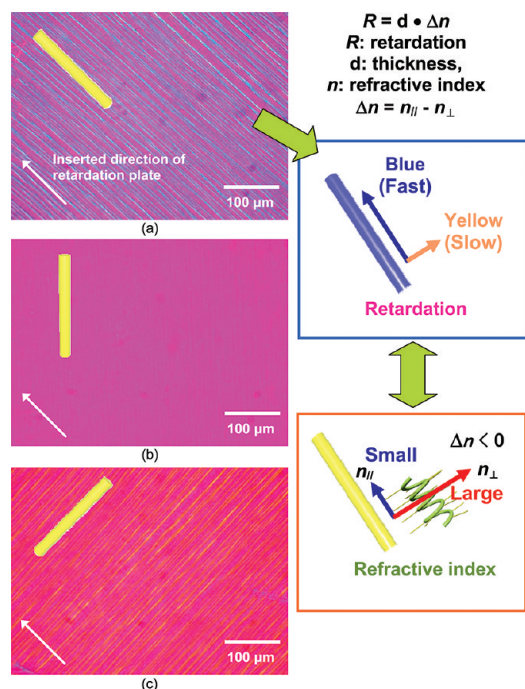


Figure 6. Interference colors of the whiskers of (*R*)-PMP observed on an oriented substrate. The whiskers are (a) parallel and (c) perpendicular to the inserted direction of first-order retardation plate ($\lambda = 530$ nm). The relative angle between the whisker and the retardation plate is (b) 45° , corresponding to the quenching position. The white arrow in the photographs indicates the inserted direction of the retardation plate, and this direction corresponds to the high refractive index of the retardation plate. The yellow bar indicates the direction of the whisker axis.

parallel to the long axis of the sample is smaller than that (n_{\perp}) perpendicular to the long axis of the sample. It also means that the sample is negatively birefringent. When the interference color is yellow, the Δn is positive, implying that n_{\parallel} is larger than n_{\perp} and hence the sample is positively birefringent.

Figure 6 depicts the interference colors of the whiskers of (*R*)-PMP observed on an oriented substrate. The interference color changed to a higher order (second-order blue) along the ordinary ray when the retardation plate was inserted parallel to the long axis of the whisker (Figure 6a).^{24,33} The rotation of the sample by 90° from the previous position changed the color to a lower order (first-order yellow) along the extraordinary ray (Figure 6c). This result indicates that the long axis of the whisker has a smaller refractive index, and the short axis (perpendicular to the long axis) a larger one. In other words, the whisker is negatively birefringent. It is worthy noting that columnar discotic liquid crystals have a larger refractive index in the horizontal plane than in the perpendicular plane.³¹ Hence, the planes of the π -stacked phenylene moieties with a larger refractive index are aligned perpendicular to the long axis of the whisker.²⁴

It is of interest to note that the polymer whiskers prepared from polyesters and π -conjugated polythiophenes have structures in which the polymer main chains self-assemble parallel to each other owing to van der Waals interactions between interchains, and they are parallel to the direction of the whiskers. On the other hand, the present whiskers prepared from helical π -conjugated PMPs have the hexagonal columnar structure in

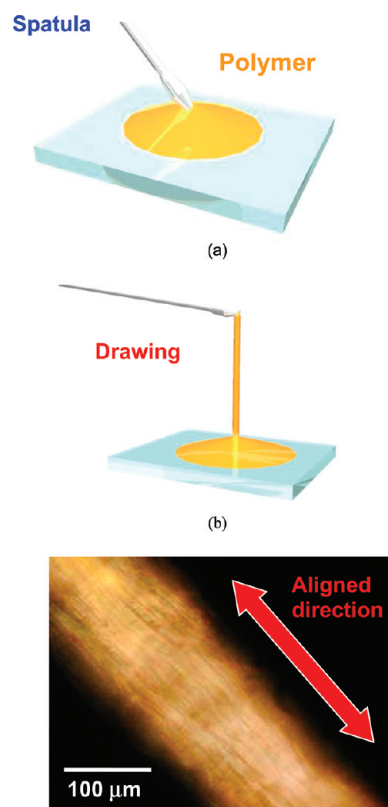


Figure 7. Method for preparation of aligned whisker bundles. (a) Polymer was cooled from an isotropic to grow whiskers at 210°C ($-0.5^\circ\text{C}/\text{min}$). (b) Polymer was aligned in the fluid state with drawing.

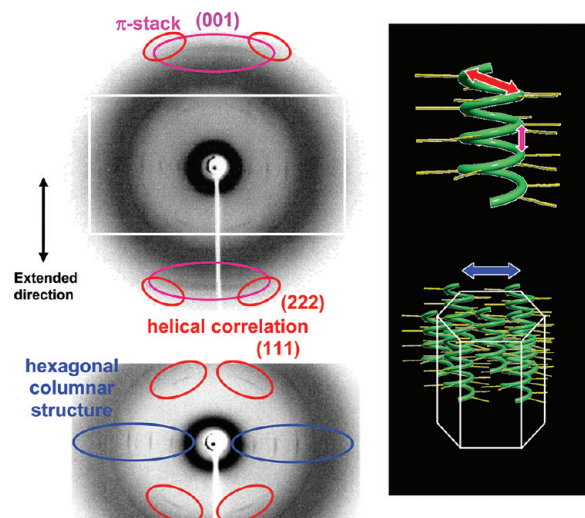


Figure 8. XRD patterns of the aligned whisker of (*R*)-PMP. The lower pattern is an enlargement of the upper one. The arrow in the figure shows the extended direction. The halos in XRD patterns are attributed to π -stack (001), helical correlation (111) and (222), and hexagonal columnar structure. The corresponding distances are indicated on the schematically described pictures of the helical polymer and the hexagonal columnar structure.

which the polymer main chain is perpendicular to the direction of the whiskers. This is quite in contrast to the polymer whiskers reported so far.

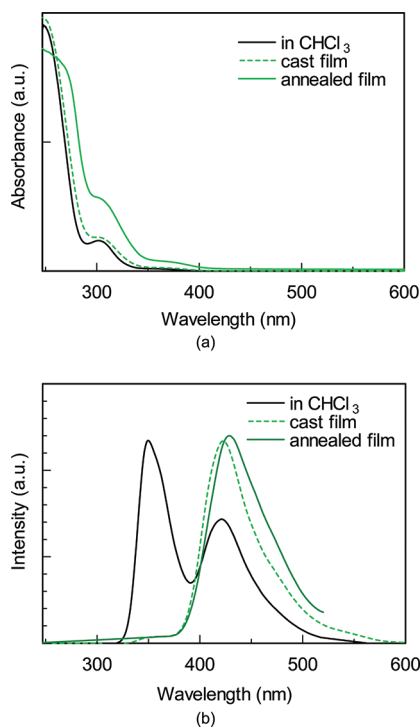


Figure 9. (a) UV–vis absorption and (b) fluorescence spectra of (*R*)-PMP in chloroform, cast film, and annealed film. The wavelength of the excitation light is 274 nm.

3.4. XRD Analysis of Aligned Whiskers. To elucidate the structure of the whisker in more detail, XRD measurements for the aligned whisker were carried out on (*R*)-PMP. The sample was prepared by drawing the polymer at an isotropic temperature to obtain the aligned polymer, and then the sample was placed in a glass capillary, as described in Figure 7. The XRD pattern of the aligned sample is shown in Figure 8.

The diffraction peaks at 23.5, 13.6, 11.8, 8.8, 7.8, 6.7, and 5.8 Å were assigned to Miller indices of (100), (110), (200), (210), (300), (310) and (400), respectively (see Figure S5 in Supporting Information). The diffractions of the hexagonal arrangement were observed perpendicular to the extended direction. The diffraction peak at 3.7 Å (001) represents the distance of the π -stacked phenylene rings and was observed parallel to the extended direction (Figure 8). This distance is consistent with the helical pitch of the polymer. The result implies that both the helical axis and the stacking order are parallel to the long axis of the whisker, and the hexagonal packing of the columns is arranged perpendicular to the long axis of the whisker. The diffraction peaks corresponding to the helical structure were observed at 7.3 Å (111). The XRD shows two pairs of the (111) diffraction intersecting the long axis of the whisker, implying a helical structure of the polymer chains. The value of 7.3 Å is in good agreement with the helix diameter (7.0 Å) calculated for the helical PMP using the molecular mechanics (MM) method.³⁴ As a consequence, it can be remarked that the whiskers are aligned to form the bundle, and the long axes of the whiskers are parallel to the aligned direction.

3.5. Optical Properties. The UV–vis and fluorescence spectra of (*R*)-PMP in chloroform, cast film and annealed film are depicted in Figure 9. Absorption band was observed at 250 nm and a shoulder at 302 nm in chloroform (Figure 9a). These bands

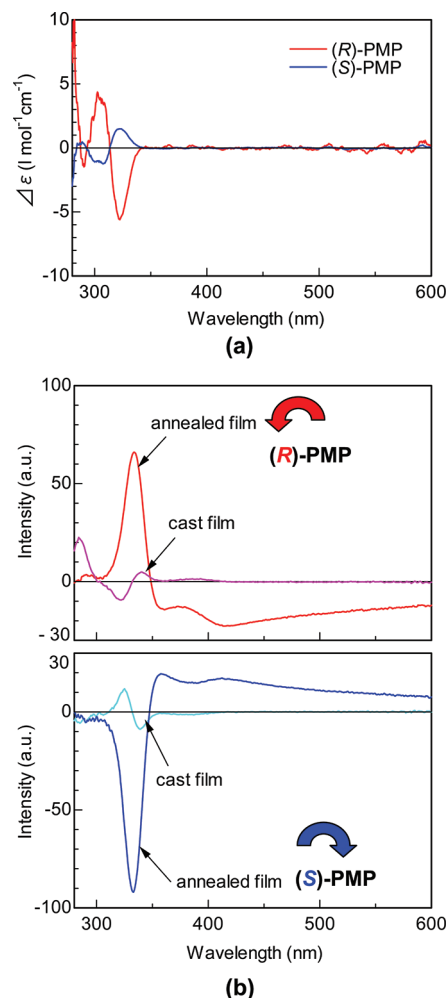


Figure 10. CD spectra of (*R*)-PMP and (*S*)-PMP in (a) chloroform and (b) the cast films (pink and light blue lines) and the annealed films (red and blue lines).

are assigned to π – π^* transition of main chain (250 nm) and that of intrachain π -stacked phenylene moiety of PMP (302 nm).

In the chloroform solution of PMP, two fluorescence bands were observed at 360 and 420 nm (Figure 9b). These bands are ascribed to fluorescence of the randomly arranged zigzag main chain (360 nm) and that of the helical main chain (420 nm). In the cast film, the fluorescence band at 420 nm increased in intensity, but the band at 360 nm was hardly observed. These results suggest that PMP in solution forms partly an intrachain helical π -stacked structure, as well as the nonhelical zigzag structure. The helical structure may be due to π -stackings between spatially adjacent phenylene moieties in the folded main chain.³⁵ Similar behavior in fluorescence due to the formation of a helical structure has been observed in a steady state for poly(phenylacetylene)s.³⁶

Figure 10 depicts CD spectra of the chiral PMPs in chloroform, cast film and annealed films. The (*R*)-PMP and (*S*)-PMP in chloroform showed bisignate CD bands with negative and positive signs in Cotton effect, respectively, at the region of 280–320 nm (Figure 10a). The bisignate CD bands may be ascribed to the exciton coupling in the intrachain helicene-like helical π -stacked phenylene moieties of the chiral PMPs. However, the CD intensities are very small, suggesting that the intrachain

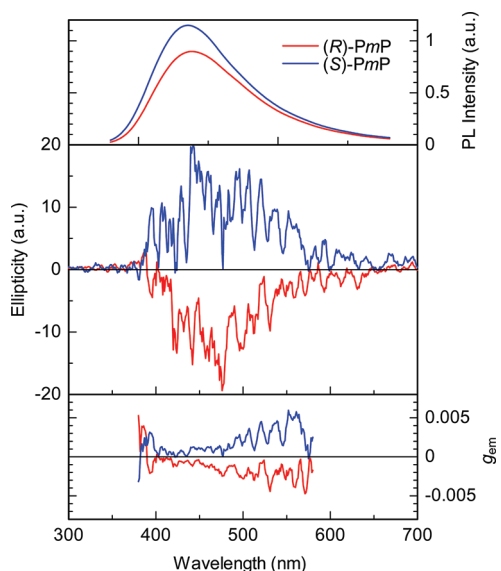


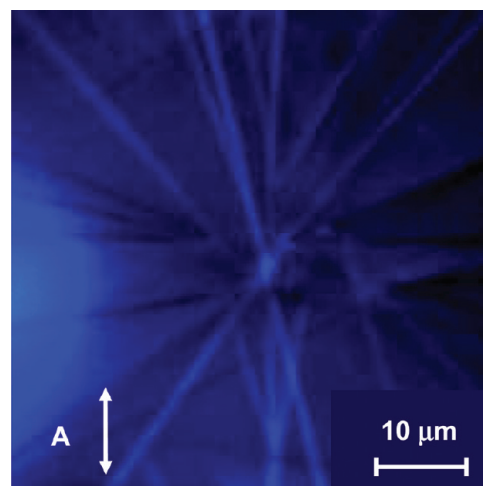
Figure 11. Spectra of fluorescence (top), circularly polarized fluorescence (CPF) (middle) and dissymmetry factor (g factor) (bottom) for annealed films of (R)-PMP and (S)-PMP. The wavelength of excited light is 274 nm. The dissymmetry factors ($|g_{em}|$) are estimated to be 1.27×10^{-3} at $\lambda = 420$ nm and 5.0×10^{-3} at $\lambda = 550$ nm.

helical π -stacked structure is loosely formed in solution, as implied by the results of UV-vis spectra (Figure 9a).

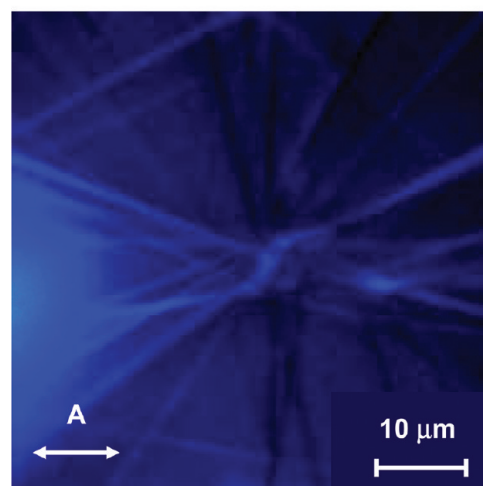
Meanwhile, the cast films of (R)-PMP and (S)-PMP showed CD bands with substantially increased intensities (Figure 10b), compared with the cases in solution. This implies that the intrachain helical π -stacking is strengthened by the self-assembly of the polymers in the cast film. However, CD bands in the cast films have opposite signs in Cotton effect to those in solution. Namely, the positive and negative bisignate Cotton effects are observed in the cast films of (R)-PMP and (S)-PMP, respectively. It remains unclear why the chiral polymer dissolved in solution and the self-assembled chiral polymers in the form of film exhibit the opposite signs in Cotton effect to each other, which should be further investigated.

In addition, the annealed films of the (R)-PMP and (S)-PMP show monosignate positive and negative CD bands with remarkably increased intensities (Figure 10b). The CD bands in the annealed films have the same signs in Cotton effect as those in the cast films. This indicates that the intrachain helical π -stacking is further strengthened by the annealing, giving rise to the highly amplified helicity in the annealed film. It should be noted that the annealed films exhibit long tails extending from 400 nm to over 800 nm, and they may be due to artifacts often observed in CD spectra for aligned films. These tails prohibited from grasping the intrinsic features of CD bands, especially from the region from 400 nm to longer wavelength. It is worthwhile to emphasize that the positive Cotton effect of the annealed film of (R)-PMP is consistent with results observed for the chromophores of M-helicity in binaphthoxyethoxys and phthalocyanines.^{27g,37,38} This supports that the (R)-PMP is stacked within the whisker and is screwed with respect to the column axis, forming a left-handed helical structure. Similarly, (S)-PMP with a negative Cotton effect should have P-helicity, i.e., a right-handed helical structure.

We also examined circularly polarized fluorescence (CPF) for (R)-PMP and (S)-PMP. Figure 11 depicts the fluorescence spectra, CPF spectra and dissymmetry factors of the polymers



(a)



(b)

Figure 12. Linearly polarized optical micrographs of (S)-PMP whiskers. The polymer shows a blue fluorescence of 420 nm when excited with a light of 365 nm. Arrows in the figures show the direction of the polarizer.

in annealed films. The dissymmetric factor in fluorescence (g_{em}) is defined as $g_{em} = 2(I_L - I_R)/(I_L + I_R) = 2\Delta I/I$, where I_L and I_R are intensities of left- and right-handed CPFs, respectively. Although the polymers in chloroform showed no CPF, the annealed polymer films showed CPFs with mirror images for (R)-PMP and (S)-PMP. The dissymmetry factor evaluated was $|g_{em}| = 1.27 \times 10^{-3}$ at 420 nm and 5.0×10^{-3} at 550 nm, which is comparable to the values reported for chiral polythiophenes ($|g_{em}| = 5.0 \times 10^{-3}$)^{1a} and smaller than those of helicenes ($|g_{em}| = 1.0 \times 10^{-2}$).^{24,39} This is probably due to less torsion between the π -stacked phenylene moieties, because the helical structure of PMP is composed of coplanar disk-like π -stacked phenylene moieties.

3.6. Linearly Polarized Luminescence. We investigated linear polarizations in fluorescence of the PMP whisker (Figure S7 in Supporting Information). Figure 12 shows the fluorescence of the annealed film of (R)-PMP when excited with a light of wavelength 365 nm. When the long axis of the whisker was parallel to the plane

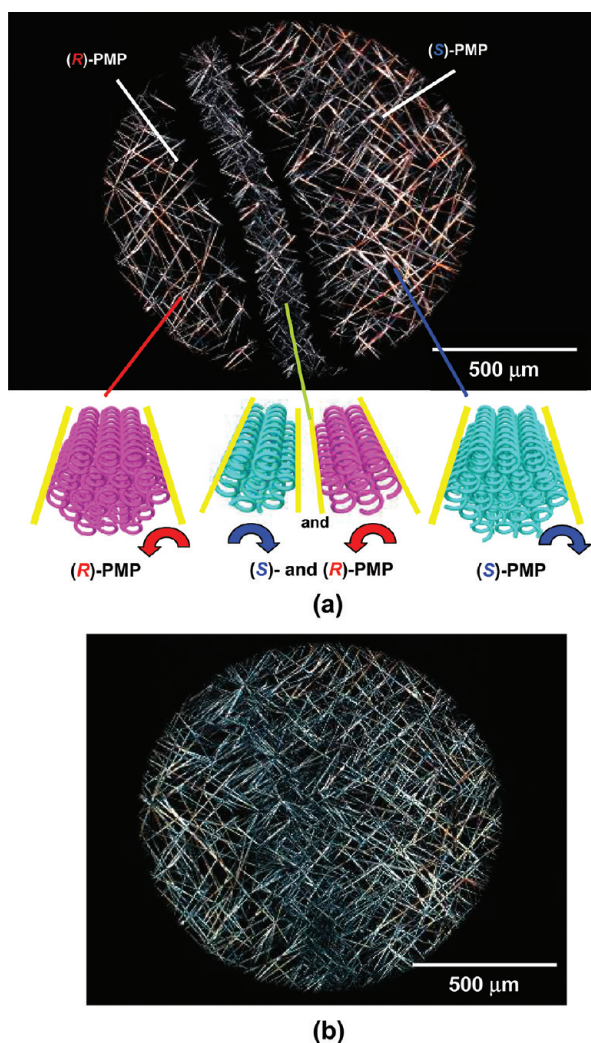


Figure 13. (a) Contact test between (*R*)-PMP and (*S*)-PMP at 204 °C. The left and right sides of the photo are (*R*)-PMP and (*S*)-PMP, respectively. The central area is the mixture of (*R*)- and (*S*)-PMP. The central area has a whisker region and two dark boundary regions. In the former (whisker region), the equimolar mixing of (*R*)- and (*S*)-PMP gives thinner and shorter whiskers. In the latter (two dark boundary region), it seems that nonequimolar mixing of (*R*)- and (*S*)-PMP depresses a grow of whisker, resulting in a dark field. (b) After cooling to 190 °C at the rate of -1 °C/min, the whiskers began to grow in the dark boundary.

of polarization of the analyzer (an angle of 0°), the blue fluorescence (420 nm) became the brightest color in the analyzer (Figure 12a). The fluorescence was quenched when the angle between the long axis and the analyzer was perpendicular (90°) (Figure 12b). These results indicate that the fluorescence at 420 nm arising from the helically π -stacked phenylene moieties is polarized along the long axis of the whisker, giving the linearly dichroic fluorescence.

3.7. Contact Test of Whiskers. To clarify the helical sense of the whiskers, we carried out contact tests of the polymers. The two polymers, (*R*)-PMP and (*S*)-PMP, were first heated to isotropic states and then cooled slowly to the temperature of 204 °C to grow the whiskers at a rate of 0.2 °C/min. Figure 13a shows a POM photograph of the contacted region between (*R*)-PMP at the left side and (*S*)-PMP at the right side. The central area in the photograph has a whisker region and two dark boundary regions.

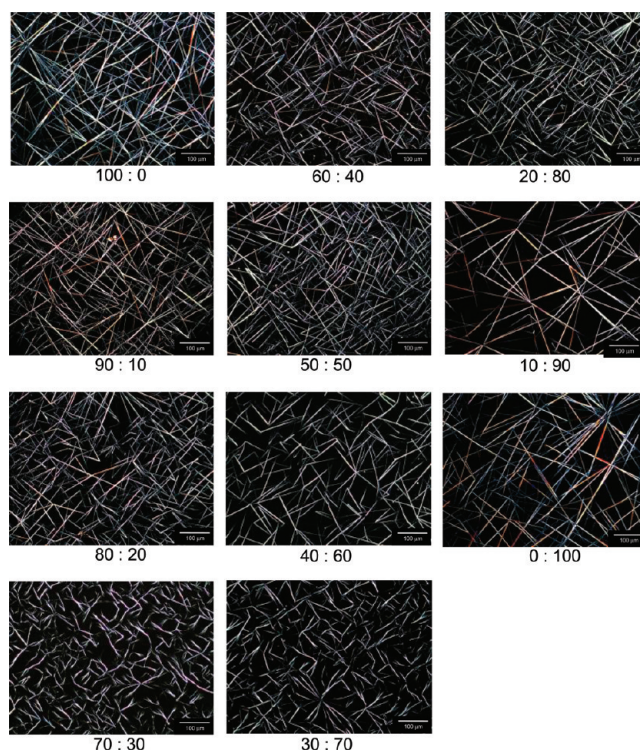


Figure 14. POM photographs of the mixtures of (*R*)-PMP and (*S*)-PMP at 190 °C. The appearance of thinner, shorter and bent whiskers in the mixing ratios of 70:30 and 30:70 [(*R*)-PMP:(*S*)-PMP] implies that a cancellation in the helical sense between two chiral polymers has occurred, and the growth of the whisker has decreased in velocity.

It is of keen interest to focus on the changes of the central area in POM; At the beginning the whole central area was yet dark, and then the whiskers gradually grew up to form the “whisker region” in the central area. However, there was still no whisker in the “dark boundary region” at this stage giving two dark boundary areas, as seen in Figure 13a. After a while, the whiskers began to grow in the dark boundary region (Figure 13b). Such changes in the central area, as well as the appearance of the dark boundary region, are due to a cancellation in the helical sense of (*R*)-PMP and (*S*)-PMP and a suppressed growing of the whiskers. Namely, (*R*)-PMP and (*S*)-PMP have opposite helical senses to each other. The whiskers formed in the boundary region consist of an equimolar mixture of chiral polymers and they are thermally less stable than those of chiral polymers, (*R*)-PMP and (*S*)-PMP. This is because the whiskers of the equimolar mixture of chiral polymers are only formed at lower temperature than 204 °C. Nevertheless, it is important to remark that not only the chiral PMPs but also the equimolar mixture of chiral PMPs form whiskers.

It is also intriguing to understand how the whisker formation is affected when the two polymers with opposite chiral configurations are mixed in various mixing ratios. The dependence of the whisker formation on the mixing ratio between (*R*)-PMP and (*S*)-PMP is examined by observing the morphological changes of the whiskers. The POM photographs of the mixtures of (*R*)-PMP and (*S*)-PMP at 190 °C are depicted in Figure 14.

The mixtures give less condensed whisker morphologies than the case of neat (*R*)-PMP or (*S*)-PMP, implying that the racemization has partly occurred to decrease the velocity of the whisker growth in the mixture. In the whisker consisting of the

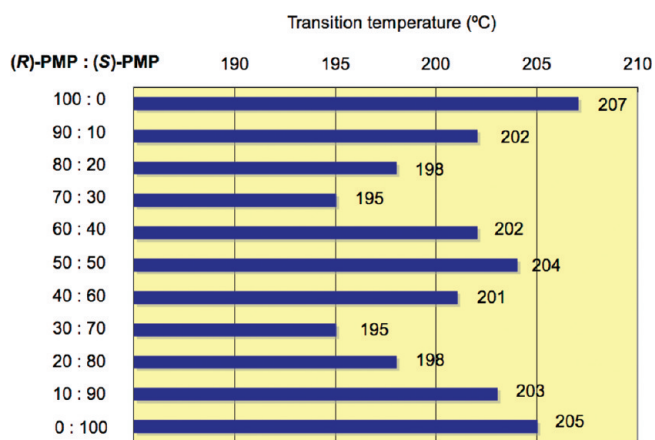


Figure 15. Transition temperature for the mixtures of (R)-PMP and (S)-PMP. The transition temperatures are determined by the points where whiskers begin to grow from isotropic phases in cooling process.

mixture of chiral polymers, a part of cancellation in helical sense between two chiral polymers should have occurred. Interestingly, the mixtures with mixing ratios of 70:30 and 30:70 [(R)-PMP:(S)-PMP] give curious whisker morphologies, where the whiskers are relatively thin and short and even bent. This result might be due to a macroscopic enantioenrichment within the whiskers, though it needs further investigation for clarification.

Figure 15 represents the transition temperatures for the mixtures of (R)-PMP and (S)-PMP. The transition temperatures are determined by the temperatures at which the whiskers begin to grow from isotropic phases in cooling process. It is found that the transition temperatures decrease with decreasing the enantiomer excess (e.e.) under the conditions from 100:0 to 70:30 in the mixing ratio for (R)-PMP:(S)-PMP, and then increase considerably for the racemate (the mixing ratio of 50:50). The transition temperatures from 50:50 through 30:70 to 0:100 give the mirror image of the above-mentioned changes. This result well explains the phenomena of the contact test between (R)-PMP and (S)-PMP as shown in Figure 13 and also the peculiar dependence of the whisker formation on the mixing ratio of the enantiomers as shown in Figure 14.

4. CONCLUSIONS

We synthesized poly(*m*-phenylene)s [PMPs] bearing chiral or achiral alkyl groups in the side chains. The PMPs synthesized by polymerizations of chiral and racemic monomers self-assemble to form whiskers, so far as the polymers bear secondary alkyl groups with appropriate lengths in side chains. The formation of the whisker is the first example among the helical π -conjugated polymers reported so far. The whiskers are composed of hexagonal columns based on the helicene-type helical π -conjugated polymers, and the columns are uniaxially packed parallel to the long axis of the whisker. The PMPs have helical structures both in solution and as solid films, and the helical structure is further enhanced in the annealed film. The chiral PMPs show not only linearly polarized fluorescence after the macroscopic alignment but also circularly polarized fluorescence owing to the helical conjugated main chain. The present whiskers have columnar hyperstructures consisting of self-assembled helical π -conjugated polymers and could be useful for prototypes of functional single fibers bearing amplified helicity.

5. EXPERIMENTAL SECTION

General Aspects. Proton (^1H) and carbon-13 (^{13}C) nuclear magnetic resonance (NMR) spectra were measured in CDCl_3 using Bruker AVANCE-500 or AVANCE-600 NMR spectrometer. Chemical shifts are represented in parts per million downfield from tetramethylsilane as an internal standard. Elemental analyses of compounds were carried out with Perkin-Elmer 2400 CHN Elemental Analyzer. Molecular weights of polymers were determined by gel permeation chromatography (GPC) using a PLgel 5 μm MIXED-D column 300×7.5 mm (Polymer Laboratories), a JASCO UV-2070 UV detector, and THF as an eluent at a flow rate of 1.0 mL/min during measurements, where the instrument was calibrated by polystyrene standard and calculated on a BORWIN integrator.

The mesomorphic properties of the polymers were evaluated using polarizing optical microscope (POM), differential scanning calorimeter (DSC), and X-ray diffraction (XRD) measurements. The polymers for the POM were sandwiched between two cover glasses. Phase transition temperatures were determined using a TA Instruments Q-100 differential scanning calorimeter (DSC) with a constant heating/cooling rate of $10^\circ\text{C}/\text{min}$ in a flowing N_2 atmosphere, while optical textures were observed under crossed polarizers using a Nikon ECLIPS E 400 POL polarizing microscope equipped with a Linkam TM 600PM heating and cooling stage. The texture of the whiskers was further examined with atomic force microscope (AFM). The samples for AFM was prepared by casting a chloroform solution of the polymer onto a glass substrate, followed by slowly cooling (about $1^\circ\text{C}/\text{min}$) from the isotropic temperature to the solid state.

Specific rotations of the monomers and polymers were measured at room temperature in chloroform using JASCO DIP-370. UV-vis absorption spectra were measured at room temperature using a Hitachi U-2000 spectrometer or a JASCO V-570. Photoluminescence spectra were recorded using a JASCO FP-750 spectrometer. Circular dichroism (CD) and circularly polarized fluorescence (CPF) spectra were measured using a JASCO J-720 and a JASCO CPL-200S spectropolarimeters, respectively. Dissymmetric factor in fluorescence (g_{em}) is defined as $g_{\text{em}} = 2(I_L - I_R)/(I_L + I_R) = 2\Delta I/I$, where I_L and I_R are fluorescence intensities of left- and right-handed circularly polarized light, respectively. All the spectroscopic measurements, UV-vis, CD, fluorescence, and CPF spectra, were performed at room temperature using a quartz cell or a quartz substrate. The films for UV-vis, CD, fluorescence, and CPF measurements were prepared by casting the chloroform solutions of the polymers on the quartz glasses. The films were heated up to 230°C and cooled to their mesophase temperatures at a rate of $1^\circ\text{C}/\text{min}$, and then cooled further to room temperature, giving annealed films. The measurement for linearly polarized fluorescence was performed with the microscope by observing the luminescent light of 420 nm through a dichroic cut filter ($\lambda = 395$ nm) and a polarizer, where the anisotropic domains were excited using an unpolarized light of 365 nm.

The samples for XRD measurements were prepared on the glass substrates by slowly cooling the polymers (about $1^\circ\text{C}/\text{min}$) from the isotropic phases to grow whiskers and then further cooling to the solid states at room temperature. XRD measurements were performed with Rigaku ultrax18HB diffractometer using a $\text{Cu K}\alpha$ irradiation ($\lambda = 1.5418$ Å), in which X-ray power was set to 12 kW. The diffraction patterns were duplicated on imaging plates, and recorded with R-Axis DS3A. The d spacing was calculated with the Bragg law of $n\lambda = 2d \sin \theta$, where n is an integer, λ is the wavelength of incident light (1.54 Å) and θ is the diffraction angle.

Molecular mechanics (MM) calculations were performed using CERIU 2 software (version 2.0; Molecular Simulations Inc., Burlington, MA) running on an Indigo2-Extreme graphics workstation (Silicon Graphics) with the supplied parameter sets. The polymer model of 10 repeating unit was built by Polymer Builder in CERIU 2 with the starting main chain conformation of *cis*-geometry.

Macroscopic alignment of the polymer was carried out by using an oriented substrate. The sample was annealed above 230 °C on the substrate which had been rubbed with a polytetrafluoroethylene (PTFE) rod at 170 °C. The refractive indices of the polymers were examined by observing a color with a retardation plate.

Ethyl-3,5-dibromobenzoate (M1, m = 2). To a suspension of 3,5-dibromobenzoic acid in ethanol (30 mL) was added 0.7 mL of concentrated H₂SO₄, and the homogenized solution was refluxed for 1 night. Then 20 mL of the solvent was removed under reduced pressure. The reaction mixture was poured into ice water. The resulting precipitate was filtered and recrystallized from an ethanol/water solution to give clear needle crystals (8.48 g, 77.0%). ¹H NMR (600 MHz, CDCl₃): δ 1.40 (t, 3H, 7.1 Hz), 4.39 (q, 2H, 7.1 Hz), 7.84 (t, 1H, 1.8 Hz), 8.10 (d, 2H, 1.8 Hz). ¹³C NMR (150 MHz, CDCl₃): δ 14.24, 61.86, 122.95, 131.31, 133.63, 137.88, 164.02. Anal. Calcd for C₉H₈Br₂O₂: C, 35.10; H, 2.62; Br, 51.89. Found: C, 35.06; H, 2.80; Br, 51.69.

1-Hexyl-3,5-dibromobenzoate (M1, m = 6). A solution of 1-hexanol (0.61 g, 5.90 mmol), 3,5-dibromobenzoic acid (1.50 g, 5.36 mmol), DCC (1.22 g, 5.90 mmol) and DMAP (0.72 g, 5.90 mmol) in dichloromethane (40 mL) was stirred at room temperature for 1 day. Then, the precipitate of DCC–urea was removed by filtration, and the solvent was removed under reduced pressure. The resulting product was purified by column chromatography (silica gel, ethyl acetate/hexane = 1/8 v/v as eluent) to give a clear oil (1.82 g, 93%). ¹H NMR (400 MHz, CDCl₃): δ 0.91 (t, 3H, 7.2 Hz), 1.34–1.44 (m, 6H), 1.76 (quint, 2H, 6.8 Hz), 4.32 (t, 2H, 6.8 Hz), 7.83 (t, 1H, 2.0 Hz), 8.08 (d, 2H, 2.0 Hz). ¹³C NMR (100 MHz, CDCl₃): δ 14.06, 22.58, 25.67, 28.62, 31.47, 66.04, 122.89, 131.21, 133.63, 138.00, 163.93. Anal. Calcd for C₁₃H₁₆Br₂O₂: C, 42.89; H, 4.43. Found: C, 42.57; H, 4.36.

1-Octyl-3,5-dibromobenzoate (M1, m = 8). A solution of 1-octanol (0.52 g, 3.93 mmol), 3,5-dibromobenzoic acid (1.00 g, 3.57 mmol), DCC (0.81 g, 3.93 mmol), and DMAP (0.48 g, 3.93 mmol) in dichloromethane (45 mL) was stirred at room temperature for 1 day. Then, the precipitate of DCC–urea was removed by filtration, and the solvent was removed under reduced pressure. The resulting product was purified by column chromatography (silica gel, ethyl acetate/hexane = 1/8 v/v as eluent) to give a clear oil (1.36 g, 97%). ¹H NMR (400 MHz, CDCl₃): δ 0.89 (t, 3H, 7.2 Hz), 1.29–1.43 (m, 10H), 1.76–1.79 (t, 2H, 7.2 Hz), 4.32 (t, 2H, 5.2 Hz), 7.83 (t, 1H, 2.0 Hz), 8.08 (d, 2H, 2.0 Hz). ¹³C NMR (100 MHz, CDCl₃): δ 14.15, 22.68, 26.00, 28.65, 31.47, 66.04, 122.89, 131.21, 133.63, 138.00, 163.93. Anal. Calcd for C₁₅H₂₀Br₂O₂: C, 45.95; H, 5.14. Found: C, 46.18; H, 5.42.

1-Decyl-3,5-dibromobenzoate (M1, m = 10). A solution of 1-decanol (0.62 g, 3.93 mmol), 3,5-dibromobenzoic acid (1.00 g, 3.57 mmol), DCC (0.81 g, 3.93 mmol), and DMAP (0.48 g, 3.93 mmol) in dichloromethane (45 mL) was stirred at room temperature for 1 day. Then, the precipitate of DCC–urea was removed by filtration, and the solvent was removed under reduced pressure. The resulting product was purified by column chromatography (silica gel, dichloromethane as eluent) to give a clear oil (1.46 g, 97%). ¹H NMR (600 MHz, CDCl₃): δ 0.88 (t, 3H, 7.1 Hz), 1.27–1.44 (m, 14H), 1.76 (quint, 2H, 7.9 Hz), 4.32 (t, 2H, 6.8 Hz), 7.84 (t, 1H, 1.8 Hz), 8.09 (d, 2H, 1.8 Hz). ¹³C NMR (150 MHz, CDCl₃): δ 14.13, 22.69, 25.95, 28.59, 29.25, 29.30, 29.50, 29.53, 31.89, 66.05, 122.97, 131.30, 133.69, 138.10, 164.08. Anal. Calcd for C₁₇H₂₄Br₂O₂: C, 48.59; H, 5.76. Found: C, 48.58; H, 5.78.

1-Hexadecyl-3,5-dibromobenzoate (M1, m = 16). A solution of 1-hexadecanol (0.58 g, 2.36 mmol), 3,5-dibromobenzoic acid (0.60 g, 2.14 mmol), DCC (0.49 g, 2.36 mmol), and DMAP (0.29 g, 2.36 mmol) in dichloromethane (20 mL) was stirred at room temperature for 1 day. Then, the precipitate of DCC–urea was removed by filtration, and the solvent was removed under reduced pressure. The resulting product was purified by column chromatography (silica gel, ethyl acetate/hexane = 1/8 v/v as eluent) to give a clear oil (1.04 g, 97%). ¹H NMR (600 MHz, CDCl₃): δ 0.88 (t, 3H, 7.1 Hz), 1.25–1.44 (m, 26H), 1.76 (quint, 2H,

7.9 Hz), 4.32 (t, 2H, 6.7 Hz), 7.84 (t, 1H, 1.8 Hz), 8.09 (d, 2H, 1.8 Hz). ¹³C NMR (150 MHz, CDCl₃): δ 14.14, 22.59, 22.71, 25.95, 28.59, 29.25, 29.38, 29.50, 29.58, 29.65, 29.67, 29.68, 29.71, 31.94, 66.05, 122.97, 131.30, 133.69, 138.10, 164.08. Anal. Calcd for C₂₃H₃₆Br₂O₂: C, 54.77; H, 7.19. Found: C, 54.87; H, 7.16.

1-Methylpentyl-3,5-dibromobenzoate (M2, m = 4). A solution of 2-hexanol (0.16 g, 1.58 mmol), 3,5-dibromobenzoic acid (0.40 g, 1.43 mmol), DCC (0.33 g, 1.58 mmol), and DMAP (0.19 g, 1.58 mmol) in dichloromethane (15 mL) was stirred at room temperature for 1 day. Then, a precipitate of DCC–urea was removed by filtration, and the solvent was removed under reduced pressure. The resulting product was purified by column chromatography (silica gel, ethyl acetate/hexane = 1/8 v/v as eluent) to give a clear oil (0.52 g, 99%). ¹H NMR (600 MHz, CDCl₃): δ 0.91 (t, 3H, 7.1 Hz), 1.31–1.38 (m, 7H), 1.68 (dm, 2H, 78.8 Hz), 5.13–5.16 (sext, 1H), 7.84 (t, 1H, 1.8 Hz), 8.09 (d, 2H, 1.8 Hz). ¹³C NMR (150 MHz, CDCl₃): δ 13.98, 20.01, 22.51, 25.62, 27.57, 35.63, 73.00, 122.93, 131.28, 134.10, 137.99, 163.62. Anal. Calcd for C₁₃H₁₆Br₂O₂: C, 42.89; H, 4.43. Found: C, 43.00; H, 4.52.

1-Methylheptyl-3,5-dibromobenzoate (M2, m = 6). A solution of 2-octanol (0.52 g, 3.93 mmol), 3,5-dibromobenzoic acid (1.00 g, 3.57 mmol), DCC (0.81 g, 3.93 mmol), and DMAP (0.48 g, 3.93 mmol) in dichloromethane (45 mL) was stirred at room temperature for 1 day. Then, a precipitate of DCC–urea was removed by filtration, and the solvent was removed under reduced pressure. The resulting product was purified by column chromatography (silica gel, ethyl acetate/hexane = 1/4 v/v as eluent) to give a clear oil (1.37 g, 98%). ¹H NMR (600 MHz, CDCl₃): δ 0.88 (t, 3H, 7.1 Hz), 1.24–1.40 (m, 11H), 1.67 (dm, 2H, 75.2 Hz), 5.15 (sext, 1H), 8.04 (t, 1H, 1.8 Hz), 8.09 (d, 2H, 1.8 Hz). ¹³C NMR (150 MHz, CDCl₃): δ 14.07, 19.99, 22.46, 25.38, 29.10, 31.69, 35.90, 73.01, 122.69, 131.27, 133.88, 137.97, 163.61. Anal. Calcd for C₁₅H₂₀Br₂O₂: C, 45.95; H, 5.14. Found: C, 45.98; H, 5.28.

1-Methyloctyl-3,5-dibromobenzoate (M2, m = 7). A solution of 2-nonanol (0.57 g, 3.93 mmol), and 40% toluene solution of DEAD (1.71 g, 3.93 mmol) in THF (10 mL) was added dropwise to a solution of 3,5-dibromobenzoic acid (1.00 g, 3.57 mmol) and TPP (1.03 g, 3.93 mmol) in THF (10 mL), and then the reaction mixture was stirred at room temperature for 48 h. The resulting solution was poured into water and extracted with dichloromethane. The organic phase was washed with water, dried over MgSO₄, and filtered. The solvent was removed under reduced pressure. The resulting product was purified by column chromatography (silica gel, dichloromethane as eluent) to give yellow oil (1.40 g, 97%). ¹H NMR (600 MHz, CDCl₃): δ 0.88 (t, 3H, 7.0 Hz), 1.22–1.40 (m, 13H), 1.67 (dm, 2H, 84 Hz), 5.14 (sext, 1H), 7.84 (t, 1H, 1.8 Hz), 8.09 (d, 2H, 1.8 Hz). ¹³C NMR (150 MHz, CDCl₃): δ 14.10, 20.00, 22.64, 25.42, 29.16, 29.38, 31.77, 35.89, 73.03, 122.93, 131.28, 134.09, 137.98, 163.63. Anal. Calcd for C₁₆H₂₂Br₂O₂: C, 47.32; H, 5.46. Found: C, 47.48; H, 5.47.

1-Methylnonyl-3,5-dibromobenzoate (M2, m = 8). A solution of 2-decanol (0.63 g, 3.93 mmol), 3,5-dibromobenzoic acid (1.00 g, 3.57 mmol), DCC (0.81 g, 3.93 mmol), and DMAP (0.48 g, 3.93 mmol) in dichloromethane (45 mL) was stirred at room temperature for 1 day. Then, a precipitate of DCC–urea was removed by filtration, and the solvent was removed under reduced pressure. The resulting product was purified by column chromatography (silica gel, ethyl acetate/hexane = 1/8 v/v as eluent) to give a clear oil (1.46 g, 81%). ¹H NMR (400 MHz, CDCl₃): δ 0.87 (t, 3H, 6.8 Hz), 0.94 (t, 3H, 7.2 Hz), 1.27–1.32 (m, 10H), 1.63–1.73 (m, 4H), 5.06 (sext, 1H), 7.83 (t, 1H, 2.0 Hz), 8.08 (d, 2H, 2.0 Hz). ¹³C NMR (100 MHz, CDCl₃): δ 9.73, 14.11, 22.63, 25.36, 27.06, 29.21, 31.73, 33.65, 77.49, 122.87, 131.18, 133.97, 137.88, 163.66; Anal. Calcd for C₁₇H₂₄Br₂O₂: C, 48.59; H, 5.76; Br, 38.03. Found: C, 48.73; H, 5.84; Br, 37.65.

1-Methyldecyl-3,5-dibromobenzoate (M2, m = 9). A solution of 2-undecanol (0.68 g, 3.93 mmol), 3,5-dibromobenzoic acid (1.00 g, 3.57 mmol), DCC (0.81 g, 3.93 mmol) and DMAP (0.48 g, 3.93 mmol) in

dichloromethane (45 mL) was stirred at room temperature for 1 day. Then, a precipitate of DCC–urea was removed by filtration, and the solvent was removed under reduced pressure. The resulting product was purified by column chromatography (silica gel, ethyl acetate/hexane = 1/4 v/v as eluent) to give a clear oil (1.54 g, 99%). ^1H NMR (600 MHz, CDCl_3): δ 0.87 (t, 3H, 7.1 Hz), 1.22–1.40 (m, 17H), 1.67 (dm, 2H, 74.6 Hz), 5.15 (sext, 1H), 7.84 (t, 1H, 1.8 Hz), 8.09 (d, 2H, 1.8 Hz). ^{13}C NMR (150 MHz, CDCl_3): δ 14.13, 20.00, 22.68, 25.41, 29.29, 29.41, 29.49, 29.51, 31.88, 35.89, 73.02, 122.92, 131.27, 134.09, 137.97, 163.61. Anal. Calcd for $\text{C}_{18}\text{H}_{26}\text{Br}_2\text{O}_2$: C, 49.79; H, 6.04. Found: C, 50.08; H, 6.25.

1-Methyldecyl-3,5-dibromobenzoate (M2, $m = 11$). A solution of 2-tridecanol (0.87 g, 4.33 mmol), 3,5-dibromobenzoic acid (1.10 g, 3.93 mmol), DCC (0.90 g, 4.33 mmol) and DMAP (0.53 g, 4.33 mmol) in dichloromethane (60 mL) was stirred at room temperature for 1 day. Then, a precipitate of DCC–urea was removed by filtration, and the solvent was removed under reduced pressure. The resulting product was purified by column chromatography (silica gel, ethyl acetate/hexane 1/8 v/v as eluent) to give a clear oil (1.59 g, 87%). ^1H NMR (600 MHz, CDCl_3): δ 0.88 (t, 3H, 7.1 Hz), 1.25–1.40 (m, 21H), 1.67 (dm, 2H, 74.5 Hz), 5.13–5.30 (sext, 1H), 7.84 (t, 1H, 1.8 Hz), 8.09 (d, 2H, 1.8 Hz). ^{13}C NMR (150 MHz, CDCl_3): δ 14.13, 20.00, 22.69, 25.41, 29.35, 29.42, 29.49, 29.56, 29.62, 29.63, 31.91, 35.90, 73.02, 122.93, 131.28, 134.11, 137.98, 163.62. Anal. Calcd for $\text{C}_{20}\text{H}_{30}\text{Br}_2\text{O}_2$: C, 51.97; H, 6.54. Found: C, 52.24; H, 6.57.

1-Ethylheptyl-3,5-dibromobenzoate (M3, $m = 8$). A solution of 3-nonanol (0.81 g, 3.93 mmol), 3,5-dibromobenzoic acid (1.00 g, 3.57 mmol), DCC (0.81 g, 3.93 mmol), and DMAP (0.48 g, 3.93 mmol) in dichloromethane (45 mL) was stirred at room temperature for 1 day. Then, a precipitate of DCC–urea was removed by filtration, and the solvent was removed under reduced pressure. The resulting product was purified by column chromatography (silica gel, ethyl acetate/hexane = 1/8 v/v as eluent) to give a clear oil (1.40 g, 97%). ^1H NMR (400 MHz, CDCl_3): δ 0.87 (t, 3H, 6.8 Hz), 1.26–1.37 (m, 13H), 1.65 (dm, 2H, 45.6 Hz), 5.14 (sext, 1H), 7.83 (t, 1H, 2.0 Hz), 8.08 (d, 2H, 2.0 Hz). ^{13}C NMR (100 MHz, CDCl_3): δ 14.16, 20.05, 22.71, 25.46, 29.27, 29.47, 31.88, 35.94, 73.01, 122.85, 131.18, 134.04, 137.88, 163.47. Anal. Calcd for $\text{C}_{16}\text{H}_{22}\text{Br}_2\text{O}_2$: C, 47.32; H, 5.46, Br, 39.35. Found: C, 47.42; H, 5.55; Br, 38.32.

1-Ethyldecyl-3,5-dibromobenzoate (M3, $m = 9$). A solution of 3-decanol (0.63 g, 3.93 mmol), 3,5-dibromobenzoic acid (1.00 g, 3.57 mmol), DCC (0.81 g, 3.93 mmol), and DMAP (0.48 g, 3.93 mmol) in dichloromethane (45 mL) was stirred at room temperature for 1 day. Then, a precipitate of DCC–urea was removed by filtration, and the solvent was removed under reduced pressure. The resulting product was purified by column chromatography (silica gel, ethyl acetate/hexane = 1/8 v/v as eluent) to give a clear oil (1.43 g, 95%). ^1H NMR (600 MHz, CDCl_3): δ 0.87 (t, 3H, 7.1 Hz), 0.94 (t, 3H, 7.4 Hz), 1.22–1.35 (m, 10H), 1.60–1.75 (m, 4H), 5.07 (quint, 1H), 7.84 (t, 1H, 1.8 Hz), 8.10 (d, 2H, 1.8 Hz). ^{13}C NMR (150 MHz, CDCl_3): δ 9.68, 14.09, 22.63, 25.34, 27.01, 29.16, 29.46, 31.77, 33.60, 77.51, 122.95, 131.28, 134.03, 137.99, 163.82. Anal. Calcd for $\text{C}_{17}\text{H}_{24}\text{Br}_2\text{O}_2$: C, 48.59; H, 5.76. Found: C, 48.89; H, 5.90.

1-Ethylundecyl-3,5-dibromobenzoate (M3, $m = 10$). A solution of 3-undecanol (0.68 g, 3.93 mmol), 3,5-dibromobenzoic acid (1.00 g, 3.57 mmol), DCC (0.81 g, 3.93 mmol) and DMAP (0.48 g, 3.93 mmol) in dichloromethane (45 mL) was stirred at room temperature for 1 day. Then, a precipitate of DCC–urea was removed by filtration, and the solvent was removed under reduced pressure. The resulting product was purified by column chromatography (silica gel, ethyl acetate/hexane = 1/4 v/v as eluent) to give a clear oil (1.55 g, 100%). ^1H NMR (600 MHz, CDCl_3): δ 0.87 (t, 3H, 7.0 Hz), 0.94 (t, 3H, 7.4 Hz), 1.25–1.34 (m, 12H), 1.59–1.73 (m, 4H), 5.07 (quint, 1H), 7.84 (t, 1H, 1.8 Hz), 8.10 (d, 2H, 1.8 Hz). ^{13}C NMR (150 MHz, CDCl_3): δ 9.68, 14.11,

22.66, 25.33, 27.01, 29.22, 29.45, 31.83, 33.59, 77.50, 122.95, 131.28, 134.03, 137.98, 163.80. Anal. Calcd for $\text{C}_{18}\text{H}_{28}\text{Br}_2\text{O}_2$: C, 49.79; H, 6.04. Found: C, 50.04; H, 6.18.

Poly[5-ethyl-*m*-benzoate] ($P1, m = 2$). To a solution of **M1** ($m = 2$) (8.00 g, 2.60 mmol) in DMF (25 mL) was added zinc powder (7.33 g, 112 mmol), 2,2'-bipyridine (0.41 g, 2.60 mmol), triphenylphosphine (2.73 g, 10.4 mmol), and nickel chloride (0.37 g, 2.60 mmol). The reaction mixture was stirred at 85 °C for 48 h, and then poured into 1 L of HCl solution (concentrated HCl/MeOH, 1/1) and stirred at room temperature for 6 h. The resulting white precipitate was filtered off, redissolved in a minimum quantity of chloroform, and poured into 1 L of MeOH to reprecipitate. After the mix was stirred for 24 h, the precipitate was filtered off to give a white solid. The precipitate was washed with disodium dihydrogen ethylenediaminetetraacetate dihydrate aq., water followed by MeOH. A sequence of the procedure was repeated three times. Yield: 2.74 g (71%). ^1H NMR (600 MHz, CDCl_3): δ 1.22–1.57 (br, 3H), 4.22–4.61 (br, 2H), 5.30–8.50 (br, 3H). Anal. Calcd for $\text{C}_9\text{H}_8\text{O}_2$: C, 72.96; H, 5.44. Found: C, 72.41; H, 5.44.

Poly[5-(1-hexyl)-*m*-benzoate] ($P1, m = 6$). To a solution of **M1** ($m = 6$) (0.71 g, 1.94 mmol) in DMF (4 mL) was added 2,2'-bipyridine (0.45 g, 2.91 mmol) and Ni(cod)₂ (0.80 g, 2.91 mmol). The reaction mixture was stirred at 100 °C for 48 h, and then poured into 500 mL of HCl solution (concentrated HCl/MeOH, 1/9) and stirred at room temperature for 2 h. The precipitate was filtered off, redissolved in a minimum quantity of THF, and poured into 500 mL of MeOH to reprecipitate. After the mix was stirred for 1 night, the precipitate was filtered to give **P1** ($m = 6$) as a white solid. Yield: 0.30 g (76%). ^1H NMR (600 MHz, CDCl_3): δ 0.84–0.98 (m, 3H), 1.22–1.53 (m, 6H), 1.64–1.91 (m, 2H), 4.29–4.67 (m, 2H), 7.86–8.20 (m, 1H), 8.25–8.53 (m, 2H). ^{13}C NMR (150 MHz, CDCl_3): δ 14.00, 22.50, 25.61, 28.64, 31.40, 65.64, 127.98, 130.65, 132.09, 141.33, 166.17. Anal. Calcd for $\text{C}_{13}\text{H}_{16}\text{O}_2$: C, 76.44; H, 7.90. Found: C, 74.45; H, 7.62.

Poly[5-(1-octyl)-*m*-benzoate] ($P1, m = 8$). To a solution of **M1** ($m = 8$) (0.65 g, 1.66 mmol) in DMF (3 mL) was added 2,2'-bipyridine (0.39 g, 2.49 mmol) and Ni(cod)₂ (0.69 g, 2.49 mmol). The reaction mixture was stirred at 80 °C for 48 h, and then poured into 500 mL of HCl solution (concentrated HCl/MeOH, 1/9) and stirred at room temperature for 2 h. The precipitate was filtered off, redissolved in a minimum quantity of THF, and poured into 500 mL of MeOH to reprecipitate. After the mix was stirred for 1 night, the precipitate was filtered to give **P1** ($m = 8$) as a white solid. Yield: 0.33 g (85%). ^1H NMR (600 MHz, CDCl_3): δ 0.80–0.90 (m, 3H), 1.19–1.64 (m, 10H), 1.76–1.90 (m, 2H), 4.36–4.46 (m, 2H), 8.13–8.17 (m, 1H), 8.31–8.57 (m, 2H). ^{13}C NMR (150 MHz, CDCl_3): δ 14.05, 22.59, 25.94, 28.69, 29.15, 29.20, 31.74, 65.65, 127.98, 130.65, 132.08, 141.33, 166.67. Anal. Calcd for $\text{C}_{15}\text{H}_{20}\text{O}_2$: C, 77.55; H, 8.68. Found: C, 76.75; H, 8.37.

Poly[5-(1-decyl)-*m*-benzoate] ($P1, m = 10$). To a solution of **M1** ($m = 10$) (0.57 g, 1.36 mmol) in DMF (4 mL) was added 2,2'-bipyridine (0.26 g, 1.64 mmol) and Ni(cod)₂ (0.45 g, 1.64 mmol). The reaction mixture was stirred at 100 °C for 72 h, and then poured into 1000 mL of HCl solution (concentrated HCl/MeOH, 1/9) and stirred at room temperature for 2 h. The precipitate was filtered off, redissolved in a minimum quantity of THF, and poured into 1000 mL of MeOH to reprecipitate. After the mix was stirred for 1 night, the precipitate was filtered to give **P1** ($m = 10$) as a brown solid. Yield: 0.42 g (88%). ^1H NMR (400 MHz, CDCl_3): δ 0.87 (br, 3H), 1.26–1.43 (m, 14H), 1.80–1.81 (br, 2H), 4.38 (br, 2H), 7.89–8.10 (m, 2H), 8.16–8.52 (m, 2H). Anal. Calcd for $\text{C}_{17}\text{H}_{26}\text{O}_2$: C, 77.82; H, 9.99. Found: C, 76.52; H, 8.57.

Poly[5-(1-hexaacyl)-*m*-benzoate] ($P1, m = 16$). To a solution of **M1** ($m = 16$) (0.70 g, 1.39 mmol) in DMF (6 mL) was added 2,2'-bipyridine (0.33 g, 2.09 mmol) and Ni(cod)₂ (0.58 g, 2.09 mmol). The reaction mixture was stirred at 80 °C for 72 h, and then poured into 300 mL of

HCl solution (concentrated HCl/MeOH, 1/9) and stirred at room temperature for 1 h. The precipitate was filtered off, redissolved in a minimum quantity of chloroform, and poured into 300 mL of MeOH to reprecipitate. After the mix was stirred for 1 night, the precipitate was filtered to give **P1** ($m = 16$) as a brown solid. Yield: 0.21 g (44%). ^1H NMR (400 MHz, CDCl_3): δ 0.83–0.86 (m, 3H), 1.21–1.41 (m, 26H), 1.80 (m, 2H), 4.37–4.45 (m, 2H), 7.92–8.13 (m, 1H), 8.30–8.58 (m, 2H). Anal. Calcd for $\text{C}_{23}\text{H}_{36}\text{O}_2$: C, 80.18; H, 10.53. Found: C, 78.90; H, 10.42.

Poly[5-(1-methylhexyl)-m-benzoate] (**P2**, $m = 4$). To a solution of **M2** ($m = 4$) (0.70 g, 1.92 mmol) in DMF (6 mL) was added 2,2'-bipyridine (0.45 g, 2.88 mmol) and $\text{Ni}(\text{cod})_2$ (0.80 g, 2.88 mmol). The reaction mixture was stirred at 60 °C for 72 h, and then poured into 300 mL of HCl solution (concentrated HCl/MeOH, 1/9) and stirred at room temperature for 2 h. The precipitate was filtered off, redissolved in a minimum quantity of THF, and poured into 300 mL of MeOH to reprecipitate. After the mix was stirred for 1 night, the precipitate was filtered to give **P2** ($m = 4$) as a white solid. Yield: 0.33 g (85%). ^1H NMR (600 MHz, CDCl_3): δ 0.86–0.96 (m, 3H), 1.26–1.46 (m, 7H), 1.61–1.88 (m, 2H), 5.18–5.30 (m, 1H), 7.86–8.13 (m, 1H), 8.28–8.54 (m, 2H). ^{13}C NMR (150 MHz, CDCl_3): δ 14.00, 14.06, 20.13, 20.19, 22.50, 22.58, 27.70, 27.77, 35.67, 72.45, 127.98, 130.70, 132.44, 141.42, 165.75. Anal. Calcd for $\text{C}_{13}\text{H}_{16}\text{O}_2$: C, 76.44; H, 7.90. Found: C, 74.31; H, 7.18.

Poly[5-(1-methylheptyl)-m-benzoate] (**P2**, $m = 6$). To a solution of **M2** ($m = 6$) (0.65 g, 1.66 mmol) in DMF (3 mL) was added 2,2'-bipyridine (0.39 g, 2.49 mmol) and $\text{Ni}(\text{cod})_2$ (0.69 g, 2.49 mmol). The reaction mixture was stirred at 100 °C for 48 h, and then poured into 500 mL of HCl solution (concentrated HCl/MeOH, 1/9) and stirred at room temperature for 2 h. The precipitate was filtered off, redissolved in a minimum quantity of chloroform, and poured into 500 mL of MeOH to reprecipitate. After the mix was stirred for 1 night, the precipitate was filtered to give **P7** as a white solid. Yield: 0.35 g (91%). ^1H NMR (400 MHz, CDCl_3): δ 0.79–0.88 (m, 3H), 1.24–1.46 (m, 11H), 1.61–1.79 (m, 2H), 5.20–5.30 (m, 1H), 7.89–8.14 (m, 1H), 8.30–8.59 (m, 2H). Anal. Calcd for $\text{C}_{15}\text{H}_{20}\text{O}_2$: C, 77.55; H, 8.68. Found: C, 77.44; H, 8.77.

Poly[5-(1-methyloctyl)-m-benzoate] (**P2**, $m = 7$). To a solution of **M2** ($m = 7$) (1.05 g, 2.59 mmol) in DMF (9 mL) was added 2,2'-bipyridine (0.61 g, 3.89 mmol) and $\text{Ni}(\text{cod})_2$ (1.07 g, 3.89 mmol). The reaction mixture was stirred at 60 °C for 48 h, and then poured into 1000 mL of HCl solution (concentrated HCl/MeOH, 1/9) and stirred at room temperature for 2 h. The precipitate was filtered off, redissolved in a minimum quantity of THF, and poured into 1000 mL of MeOH to reprecipitate. After the mix was stirred for 1 night, the precipitate was filtered to give **P2** ($m = 7$) as a white solid. Yield: 0.47 g (74%). ^1H NMR (400 MHz, CDCl_3): δ 0.80–0.86 (m, 3H), 1.24–1.45 (m, 10H), 1.56–1.77 (m, 2H), 5.21–5.22 (m, 1H), 7.92–8.10 (m, 1H), 8.30–8.53 (m, 2H). Anal. Calcd for $\text{C}_{16}\text{H}_{24}\text{O}_2$: C, 77.38; H, 9.74. Found: C, 77.52; H, 8.83.

Poly[5-(1-methynonyl)-m-benzoate] (**P2**, $m = 8$). To a solution of **M2** ($m = 8$) (0.65 g, 1.60 mmol) in DMF (6 mL) was added 2,2'-bipyridine (0.38 g, 2.40 mmol) and $\text{Ni}(\text{cod})_2$ (0.66 g, 2.40 mmol). The reaction mixture was stirred at 80 °C for 48 h and then poured into 300 mL of HCl solution (concentrated HCl/MeOH, 1/9) and stirred at room temperature for 2 h. The precipitate was filtered off, redissolved in a minimum quantity of THF, and poured into 300 mL of MeOH to reprecipitate. After the mix was stirred for 1 night, the precipitate was filtered to give **P2** ($m = 8$) as a white solid. Yield: 0.33 g (83%). ^1H NMR (400 MHz, CDCl_3): δ 0.79–0.85 (m, 3H), 1.20–1.45 (m, 15H), 1.58–1.88 (m, 2H), 5.19–5.30 (m, 1H), 7.88–8.11 (m, 1H), 8.30–8.58 (m, 2H). Anal. Calcd for $\text{C}_{17}\text{H}_{24}\text{O}_2$: C, 78.42; H, 9.29. Found: C, 77.52; H, 9.10.

Poly[5-(1-methyldecyl)-m-benzoate] (**P2**, $m = 9$). To a solution of **M2** ($m = 9$) (0.65 g, 1.50 mmol) in DMF (6 mL) was added 2,2'-bipyridine

(0.36 g, 2.25 mmol) and $\text{Ni}(\text{cod})_2$ (0.62 g, 2.25 mmol). The reaction mixture was stirred at 100 °C for 48 h and then poured into 500 mL of HCl solution (concentrated HCl/MeOH, 1/9) and stirred at room temperature for 2 h. The precipitate was filtered off, redissolved in a minimum quantity of THF, and poured into 500 mL of MeOH to reprecipitate. After the mix was stirred for 1 night, the precipitate was filtered to give **P2** ($m = 9$) as a white solid. Yield: 0.33 g (81%). ^1H NMR (400 MHz, CDCl_3): δ 0.80–0.85 (m, 3H), 1.19–1.45 (m, 17H), 1.63–1.86 (m, 2H), 5.21–5.31 (m, 1H), 7.88–8.12 (m, 1H), 8.30–8.58 (m, 2H). Anal. Calcd for $\text{C}_{18}\text{H}_{26}\text{O}_2$: C, 78.79; H, 9.55. Found: C, 78.05; H, 9.38.

Poly[5-(1-methyldodecyl)-m-benzoate] (**P2**, $m = 11$). To a solution of **M2** ($m = 11$) (0.70 g, 1.51 mmol) in DMF (6 mL) was added 2,2'-bipyridine (0.36 g, 2.27 mmol) and $\text{Ni}(\text{cod})_2$ (0.63 g, 2.27 mmol). The reaction mixture was stirred at 60 °C for 48 h and then poured into 300 mL of HCl solution (concentrated HCl/MeOH, 1/9) and stirred at room temperature for 2 h. The precipitate was filtered off, redissolved in a minimum quantity of THF, and poured into 300 mL of MeOH to reprecipitate. After the mix was stirred for 1 night, the precipitate was filtered to give **P2** ($m = 11$) as a white solid. Yield: 0.42 g (93%). ^1H NMR (600 MHz, CDCl_3): δ 0.81–0.86 (m, 3H), 1.11–1.45 (m, 21H), 1.60–1.85 (m, 2H), 5.22–5.31 (m, 1H), 7.86–8.22 (m, 1H), 8.31–8.53 (m, 2H). ^{13}C NMR (150 MHz, CDCl_3): δ 14.10, 20.12, 22.66, 25.58, 29.32, 29.44, 29.53, 29.61, 31.87, 36.00, 72.45, 127.99, 130.67, 132.44, 141.42, 165.73. Anal. Calcd for $\text{C}_{20}\text{H}_{30}\text{O}_2$: C, 79.42; H, 10.00. Found: C, 78.02; H, 9.14.

Poly[5-(1-ethylheptyl)-m-benzoate] (**P3**, $m = 8$). To a solution of **M3** ($m = 8$) (0.65 g, 1.60 mmol) in DMF (6 mL) was added 2,2'-bipyridine (0.38 g, 2.40 mmol) and $\text{Ni}(\text{cod})_2$ (0.66 g, 2.40 mmol). The reaction mixture was stirred at 80 °C for 48 h and then poured into 300 mL of HCl solution (concentrated HCl/MeOH, 1/9) and stirred at room temperature for 1 h. The precipitate was filtered off, redissolved in a minimum quantity of chloroform, and poured into 300 mL of MeOH to reprecipitate. After the mix was stirred for 1 night, the precipitate was filtered to give **P3** ($m = 8$) as a white solid. Yield: 0.32 g (79%). ^1H NMR (400 MHz, CDCl_3): δ 0.79–0.87 (m, 3H), 0.94–1.06 (m, 3H), 1.23–1.31 (m, 8H), 1.64–1.83 (m, 4H), 5.12–5.23 (m, 1H), 7.90–8.15 (m, 1H), 8.32–8.60 (m, 2H). Anal. Calcd for $\text{C}_{16}\text{H}_{22}\text{O}_2$: C, 78.01; H, 9.00. Found: C, 77.23; H, 9.05.

Poly[5-(1-ethyloctyl)-m-benzoate] (**P3**, $m = 9$). To a solution of **M3** ($m = 9$) (0.65 g, 1.55 mmol) in DMF (6 mL) was added 2,2'-bipyridine (0.37 g, 2.33 mmol) and $\text{Ni}(\text{cod})_2$ (0.64 g, 2.33 mmol). The reaction mixture was stirred at 100 °C for 48 h and then poured into 500 mL of HCl solution (concentrated HCl/MeOH, 1/9) and stirred at room temperature for 2 h. The precipitate was filtered off, redissolved in a minimum quantity of chloroform, and poured into 500 mL of MeOH to reprecipitate. After the mix was stirred for 1 night, the precipitate was filtered to give **P3** ($m = 9$) as a white solid. Yield: 0.32 g (78%). ^1H NMR (400 MHz, CDCl_3): δ 0.78–0.87 (m, 3H), 0.94–1.06 (m, 3H), 1.20–1.47 (m, 10H), 1.64–1.83 (m, 4H), 5.12–5.23 (m, 1H), 7.90–8.14 (m, 1H), 8.32–8.60 (m, 2H). Anal. Calcd for $\text{C}_{17}\text{H}_{24}\text{O}_2$: C, 78.42; H, 9.29. Found: C, 77.95; H, 9.18.

Poly[5-(1-ethynonyl)-m-benzoate] (**P3**, $m = 10$). To a solution of **M3** ($m = 10$) (0.65 g, 1.50 mmol) in DMF (6 mL) was added 2,2'-bipyridine (0.36 g, 2.25 mmol) and $\text{Ni}(\text{cod})_2$ (0.62 g, 2.25 mmol). The reaction mixture was stirred at 100 °C for 48 h and then poured into 500 mL of HCl solution (concentrated HCl/MeOH, 1/9) and stirred at room temperature for 2 h. The precipitate was filtered off, redissolved in a minimum quantity of chloroform, and poured into 500 mL of MeOH to reprecipitate. After the mix was stirred for 1 night, the precipitate was filtered to give **P3** ($m = 10$) as a white solid. Yield: 0.41 g (99%). ^1H NMR (400 MHz, CDCl_3): δ 0.79–0.85 (m, 3H), 0.94–1.06 (m, 3H), 1.25–1.46 (m, 12H), 1.62–1.84 (m, 4H), 5.13–5.23 (m, 1H), 7.93–8.14 (m, 1H), 8.32–8.60 (m, 2H). Anal. Calcd for $\text{C}_{18}\text{H}_{26}\text{O}_2$: C, 78.79; H, 9.55. Found: C, 78.88; H, 9.64.

(R)-(-)-1-Methyloctyl-3,5-dibromobenzoate [(R)-M2, $m = 7$]. (S)-(+)-2-Nonanol (4.10 g, 29.0 mmol) and DEAD (5.00 g, 40 wt % in toluene, 29.0 mmol) dissolved in THF (10 mL) was added dropwise to a solution of 3,5-dibromobenzoic acid (8.00 g, 29.0 mmol) and TPP (7.50 g, 29.0 mmol) in THF (20 mL). The mixture was stirred for 48 h at 60 °C under an argon atmosphere. The solution was poured into water and extracted with dichloromethane. The organic phase was washed with water, dried over MgSO_4 , and filtered. The solvent was removed under reduced pressure, and the residue was purified by column chromatography (silica gel, dichloromethane as eluent) to give yellow oil (8.6 g, 74%). ^1H NMR (600 MHz, CDCl_3): δ 0.88 (t, 3H, 7 Hz), 1.36–1.25 (m, 12H), 1.66 (d, 3H, 53 Hz), 5.14 (sext, 1H, 6 Hz), 7.83 (s, 1H), 8.08 (s, 2H). ^{13}C NMR (150 MHz, CDCl_3): δ 14.1, 20.0, 22.6, 25.4, 29.2, 29.4, 31.8, 35.9, 73.0, 122.9, 131.3, 134.1, 138.0, 163.6; Anal. Calcd for $\text{C}_{23}\text{H}_{29}\text{NO}_2$: C, 47.3; H, 5.46. Found: C, 47.0; H 5.53. $[\alpha]_{\text{D}}^{22} = -25.9^\circ$ ($c = 1.0$ in chloroform).

(S)-(+)-1-Methyloctyl-3,5-dibromobenzoate [(S)-M2, $m = 7$]. The titled compound was prepared from 2-nonanol (5.7 g, 40 mmol), DEAD (17 g, 40 mmol), 3,5-dibromobenzoic acid (11 g, 40 mmol), and TPP (10 g, 40 mmol) in THF (40 mL), using the same procedure as that for (R)-(-)-1-methyloctyl-3,5-dibromobenzoate. Yield: 12 g (74%). ^1H NMR (600 MHz, CDCl_3): δ 0.90 (t, 3H, 7 Hz), 1.39–1.29 (m, 12H), 1.70 (d, 3H, 68 Hz), 5.17 (sext, 1H, 6 Hz), 7.86 (s, 1H), 8.11 (s, 2H). ^{13}C NMR (150 MHz, CDCl_3): δ 14.1, 20.0, 22.6, 25.4, 29.2, 29.4, 31.8, 35.9, 73.0, 122.9, 131.3, 134.1, 138.0, 163.6. Anal. Calcd for $\text{C}_{23}\text{H}_{29}\text{NO}_2$: C, 47.3; H, 5.46. Found: C, 47.0; H, 5.36. $[\alpha]_{\text{D}}^{22} = +23.9^\circ$ ($c = 1.0$ in chloroform).

Poly{5-[(R)-(-)-1-methyloctyl]-*m*-benzoate} [(R)-PMP, $m = 7$]. A mixture of DMF (5 mL) and 2,2'-bipyridine, bpy (0.94 g, 6.02 mmol), and Ni(COD)₂ (COD: cyclooctadiene) (1.65 g, 6.00 mmol) was stirred at room temperature for 30 min under an argon atmosphere, and then (R)-(-)-1-methyloctyl-3,5-dibromobenzoate (2.10 g, 5.17 mmol) dissolved in 5 mL of DMF was added to it. The mixture was stirred at 100 °C for 48 h. The reaction mixture was cooled to room temperature, poured into a large amount of a mixture of 12 M hydrochloric acid and methanol (1:9, 1000 mL), and vigorously stirred for 2 h. The resulting precipitate was collected by filtration and dissolved in a minimum amount of THF. The insoluble part was removed by filtration, and the filtrate was reprecipitated in methanol (1000 mL). After stirring for 24 h, the resulting precipitate was collected by filtration. (R)-PMP was obtained as a brown solid (1.28 g, 99%). ^1H NMR (600 MHz, CDCl_3): δ 0.81 (t, 3H, 7 Hz), 1.37–1.13 (m, 12H), 1.71 (d, 3H, 80 Hz), 5.22 (sext, 1H, 6 Hz), 8.11 (s, 1H), 8.35 (s, 2H). ^{13}C NMR (125 MHz, CDCl_3): δ 14.4, 20.5, 23.0, 26.0, 29.5, 29.8, 32.1, 36.4, 72.8, 128.4, 131.1, 132.9, 141.8, 166.1. Anal. Calcd for $\text{C}_{23}\text{H}_{29}\text{NO}_2$: C, 77.4; H, 9.74. Found: C, 77.4; H, 8.55. $[\alpha]_{\text{D}}^{22} = -65.2^\circ$ ($c = 1.0$ in chloroform).

Poly{5-[(S)-(+)-1-methyloctyl]-*m*-benzoate} [(S)-PMP, $m = 7$]. The titled polymer was prepared from (S)-(+)-1-methyloctyl-3,5-dibromobenzoate (2.10 g, 5.17 mmol), 2,2'-bipyridine (0.94 g, 6.02 mmol), and Ni(cod)₂ (1.65 g, 6.00 mmol) in DMF (10 mL), with the same procedure as that for poly{5-[(R)-(-)-1-methyloctyl]-*m*-phenylbenzoate}. Yield: 1.25 g (97%). ^1H NMR (600 MHz, CDCl_3): δ 0.81 (t, 3H, 7 Hz), 8.35 (s, 2H), 1.37–1.13 (m, 12H), 1.71 (d, 3H, 78 Hz), 5.22 (sext, 1H, 6 Hz), 8.11 (s, 1H), 8.35 (s, 2H). ^{13}C NMR (125 MHz, CDCl_3): δ 14.4, 20.5, 23.0, 25.9, 29.5, 29.8, 32.2, 36.4, 72.8, 128.4, 131.1, 132.9, 141.8, 166.1. Anal. Calcd for $\text{C}_{23}\text{H}_{29}\text{NO}_2$: C, 77.4; H, 9.74. Found: C, 77.4; H, 8.55. $[\alpha]_{\text{D}}^{23} = +67.9^\circ$ ($c = 1.0$ in chloroform).

ASSOCIATED CONTENT

Supporting Information. Atomic force micrograph (AFM) and X-ray diffraction (XRD) of the polymers and the method for measurement of the refractive index. This material is available free of charge via the Internet at <http://pubs.acs.org>.

AUTHOR INFORMATION

Corresponding Author

*E-mail: akagi@fps.polym.kyoto-u.ac.jp.

ACKNOWLEDGMENT

We thank Mr. Jun Yoshida for his helpful cooperation in polarized optical microscope measurements.

This work is supported by a Grant-in-Aid for Science Research (S) (No. 20225007) from the Ministry of Education, Culture, Sports, Science and Technology, Japan.

REFERENCES

- (1) (a) Yamashita, Y.; Kato, Y.; Endo, S.; Kimura, K. *Makromol. Chem. Rapid Commun.* **1988**, *9*, 687. (b) Kimura, K.; Kato, Y.; Inabe, T.; Yamashita, Y. *Macromolecules* **1995**, *28*, 255.
- (2) Ihn, K. J.; Moulton, J.; Smith, P. J. *Polym. Sci., Part B: Polym. Phys.* **1993**, *31*, 735.
- (3) (a) Langeveld-Voss, B. M. W.; Janssen, R. A. J.; Christiaans, M. P. T.; Meskers, S. C. J.; Dekkers, H. P. J. M.; Meijer, E. W. J. *Am. Chem. Soc.* **1996**, *118*, 4908. (b) Oda, M.; Nothofer, H.-G.; Lieser, G.; Scherf, U.; Meskers, S. C. J.; Neher, D. *Adv. Mater.* **2000**, *12*, 362.
- (4) (a) Sinclair, M.; Moses, D.; Akagi, K.; Heeger, A. J. *Phys. Rev. B* **1988**, *38*, 10724. (b) In *Electrical and Optical Polymer Systems: Fundamentals, Methods, and Applications*; Wise, D. L.; Wnek, G. E.; Trantolo, D. J.; Cooper, T. M.; Gresser, J. D., Eds.; Marcel Dekker: New York, 1998.
- (5) Suh, D. S.; Kim, T. J.; Aleshin, A. N.; Park, Y. W.; Piao, G.; Akagi, K.; Shirakawa, H.; Qualls, J. S.; Han, S. Y.; Brooks, J. S. *J. Chem. Phys.* **2001**, *114*, 7222.
- (6) (a) Akagi, K.; Piao, G.; Kaneko, S.; Sakamaki, K.; Shirakawa, H.; Kyotani, M. *Science* **1998**, *282*, 1683. (b) Akagi, K. *Chem. Rev.* **2009**, *109*, 5354.
- (7) Cheuk, K. K. L.; Lam, J. W. Y.; Tang, B. Z. *Polym. Mater. Sci. Eng.* **2000**, *82*, 56.
- (8) (a) Kang, E. T.; Ehrlich, P.; Bhatt, A. P.; Anderson, W. A. *Macromolecules* **1984**, *17*, 1020. (b) Yashima, E.; Maeda, K.; Okamoto, Y. *Nature* **1999**, *399*, 449.
- (9) Bouman, M. M.; Meijer, E. W. *Adv. Mater.* **1995**, *7*, 385.
- (10) (a) Khan, A.; Müller, S.; Hecht, S. *Chem. Commun.* **2005**, 584. (b) Vanormelingen, W.; Pandey, L.; Van der Auweraer, M.; Verbiest, T.; Koeckelberghs, G. *Macromolecules* **2010**, *43*, 2157.
- (11) (a) Green, M. M.; Peterson, N. C.; Sato, T.; Teramoto, A.; Cook, R.; Lifson, S. *Science* **1995**, *268*, 1860. (b) Dai, Y.; Katz, T. J.; Nichols, D. A. *Angew. Chem., Int. Ed. Engl.* **1996**, *35*, 2109. (c) Suda, K.; Yoshida, J.; Nimori, S.; Akagi, K. *Synth. Met.* **2009**, *159*, 943.
- (12) (a) Nelson, J. C.; Saven, J. G.; Moore, J. S.; Wolynes, P. G. *Science* **1997**, *277*, 1793. (b) Kubel, C.; Mio, M. J.; Moore, J. S.; Martin, D. C. *J. Am. Chem. Soc.* **2002**, *124*, 8605.
- (13) Williams, D. J.; Colquhoun, H. M.; Mahoney, C. A. O. *Chem. Commun.* **1994**, 1643.
- (14) Kobayashi, N.; Sasaki, S.; Abe, M.; Watanabe, S.; Fukumoto, H.; Yamamoto, T. *Macromolecules* **2004**, *37*, 7986.
- (15) Schunn, R. A. *Inorg. Synth.* **1974**, *15*, 5.
- (16) (a) Mitsunobu, O. *Synthesis* **1981**, 1. (b) Kasthuraiah, N.; Sadashira, B. K.; Krishnaprasad, S.; Nair, G. G. *J. Mater. Chem.* **1996**, *6*, 1619. (c) Svensson, M.; Helgee, B.; Skarp, K.; Anderson, G. *J. Mater. Chem.* **1998**, *8*, 353.
- (17) (a) Yamamoto, T.; Morita, A.; Miyazaki, Y.; Maruyama, T.; Wakayama, H.; Zhou, Z. H.; Nakamura, Y.; Kanbara, T.; Sasaki, S. *Macromolecules* **1996**, *29*, 7432. (b) Kaeriyama, K.; Kouyama, S.; Sekita, M.; Nakayama, T.; Tsukahara, Y. *Macromol. Rapid Commun.* **1999**, *20*, 50.
- (18) (a) Kelly, S. M. *Liq. Cryst.* **1996**, *20*, 493. (b) Dyer, D. J.; Walba, D. M. *Chem. Mater.* **1994**, *6*, 1096.
- (19) Lai, C. K.; Tsai, C.-H.; Pang, Y.-S. *J. Mater. Chem.* **1998**, *8*, 1335.

- (20) (a) Dahn, U.; Erdelen, C.; Ringsdorf, H.; Festag, R.; Wendorff, J. H.; Heiney, P. A.; Maliszewskij, N. C. *Liq. Cryst.* **1995**, *19*, 759. (b) Barbera, J.; Garcès, A. C.; Jayaramam, N.; Omenat, A.; Serrano, J. L.; Stoddart, J. F. *Adv. Mater.* **2001**, *13*, 175.
- (21) Nuckolls, C.; Katz, T. J. *J. Am. Chem. Soc.* **1998**, *120*, 9541.
- (22) (a) Livolant, F.; Levelut, A. M.; Doucet, J.; Benoit, J. P. *Nature* **1989**, *339*, 724. (b) Bushey, M. L.; Hwang, A.; Stephens, P. W.; Nuckolls, C. *J. Am. Chem. Soc.* **2001**, *123*, 8157.
- (23) Phillips, K. E. S.; Katz, T. J.; Jockusch, S.; Lovinger, A. J.; Turro, N. J. *J. Am. Chem. Soc.* **2001**, *123*, 11899.
- (24) Lovinger, A. J.; Nuckolls, C.; Katz, T. J. *J. Am. Chem. Soc.* **1998**, *120*, 264.
- (25) Mohr, B.; Wegner, G.; Ohta, K. *Chem. Commun.* **1995**, 995.
- (26) Kang, S. H.; Kang, Y.-S.; Zin, W.-C.; Olbrechts, G.; Clays, K.; Persoons, A.; Kim, K. *Chem. Commun.* **1999**, 1661.
- (27) (a) Seo, J.-S.; Yoo, Y.-S.; Choi, M.-G. *J. Mater. Chem.* **2001**, *11*, 1332. (b) Kumar, S.; Wachtel, E. J.; Keinan, E. *J. Org. Chem.* **1993**, *58*, 3821. (c) Lee, H.-K.; Lee, H.; Ko, Y. H.; Chang, Y. J.; Oh, N.-K.; Zin, W.-C.; Kim, K. *Angew. Chem., Int. Ed.* **2001**, *40*, 2669. (d) Lee, M.; Lee, D.-W.; Cho, B.-K. *J. Am. Chem. Soc.* **1998**, *120*, 13258. (e) Fisher, H.; Ghosh, S. S.; Heiney, P. A.; Maliszewskij, N. C.; Plesniviy, T.; Ringsdorf, H.; Seitz, M. *Angew. Chem., Int. Ed.* **1995**, *34*, 795. (f) Sauer, T. *Macromolecules* **1993**, *26*, 2057. (g) Brunsveld, L.; Prince, R. B.; Meijer, E. W.; Moore, J. S. *Org. Lett.* **2000**, *2*, 1525. (h) Destrade, C.; Nguyen, H. T.; Gasparoux, H.; Malthête, J.; Levelut, A. M. *Mol. Cryst. Liq. Cryst.* **1981**, *71*, 111.
- (28) Boden, N.; Bushby, R. J.; Jesudason, M. V.; Sheldrick, B. *Chem. Commun.* **1988**, 1342.
- (29) (a) Castella, M.; López-calahorra, F.; Velasco, D. *Liq. Cryst.* **2002**, *29*, 559. (b) Ohta, K.; Ando, N.; Yamamoto, I. *Liq. Cryst.* **1999**, *26*, 663.
- (30) Lehn, J.-M.; Malthête, J.; Levelut, A.-M. *Chem. Commun.* **1985**, 1794.
- (31) Pisula, W.; Kastler, M.; Wasserfallen, D.; Pakula, T.; Müllen, K. *J. Am. Chem. Soc.* **2004**, *126*, 8074.
- (32) Lehn, J.-M.; Malthête, J.; Levelut, A.-M. *Chem. Commun.* **1985**, 1794.
- (33) (a) Livolant, F.; Levelut, A. M.; Doucet, J.; Benoit, J. P. *Nature* **1989**, *339*, 724. (b) Bushey, M. L.; Hwang, A.; Stephens, P. W.; Nuckolls, C. *J. Am. Chem. Soc.* **2001**, *123*, 157.
- (34) (a) Fontes, E.; Heiney, P. A.; de Jeu, W. H. *Phys. Rev. Lett.* **1988**, *61*, 1202. (b) van der Pol, J. F.; Neeleman, E.; Zwikker, J. W.; Nolte, R. J. M.; Drenth, W.; Aerts, J.; Visser, R.; Picken, S. J. *Liq. Cryst.* **1989**, *6*, 577. (c) Engel, M. K.; Bassoul, P.; Bosio, L.; Lehmann, H.; Hanack, M.; Simon, J. *Liq. Cryst.* **1993**, *15*, 709.
- (35) (a) Hanan, G. S.; Lehn, J.-M.; Kyritsakas, N.; Fischer, J. *Chem. Commun.* **1995**, 765. (b) Bassani, D. M.; Lehn, J.-M. *Bull. Soc. Chim. Fr.* **1997**, *134*, 897.
- (36) (a) Prince, R. B.; Saven, J. G.; Wolynes, P. G.; Moore, J. S. *J. Am. Chem. Soc.* **1999**, *121*, 3114. (b) Yang, W. Y.; Prince, R. B.; Sabelko, J.; Moore, J. S.; Gruebele, M. *J. Am. Chem. Soc.* **2000**, *122*, 3248.
- (37) (a) Kobayashi, N.; Kobayashi, Y.; Osa, T. *J. Am. Chem. Soc.* **1993**, *115*, 10994. (b) Fox, J. M.; Katz, T. J.; Elshocht, S. V.; Verbiest, T.; Kauranen, M.; Persoons, A.; Thongpanchang, T.; Krauss, T.; Brus, L. *J. Am. Chem. Soc.* **1999**, *121*, 3453.
- (38) Nuckolls, C.; Katz, T. J.; Katz, G.; Collings, P. J.; Castellanos, L. *J. Am. Chem. Soc.* **1999**, *121*, 79.
- (39) (a) Verbiest, T.; Van Elshocht, S.; Kauranen, M.; Hellemans, L.; Snauwaert, J.; Nuckolls, C.; Katz, T. J.; Persoons, A. *Science* **1998**, *282*, 913. (b) Sioncke, S.; Van Elshocht, S.; Verbiest, T.; Persoons, A.; Mauranen, M.; Phillips, K. E. S.; Katz, T. J. *J. Chem. Phys.* **2000**, *113*, 7578.